



2011

## Role for Histone Deacetylases in Glucocorticoid Receptor Mediated Transpression of Natural Killer Cell Activity

Kristin Bush  
*Loyola University Chicago*

Follow this and additional works at: [https://ecommons.luc.edu/luc\\_theses](https://ecommons.luc.edu/luc_theses)

 Part of the [Immunology and Infectious Disease Commons](#)

---

### Recommended Citation

Bush, Kristin, "Role for Histone Deacetylases in Glucocorticoid Receptor Mediated Transpression of Natural Killer Cell Activity" (2011). *Master's Theses*. 567.  
[https://ecommons.luc.edu/luc\\_theses/567](https://ecommons.luc.edu/luc_theses/567)

This Thesis is brought to you for free and open access by the Theses and Dissertations at Loyola eCommons. It has been accepted for inclusion in Master's Theses by an authorized administrator of Loyola eCommons. For more information, please contact [ecommons@luc.edu](mailto:ecommons@luc.edu).



This work is licensed under a [Creative Commons Attribution-Noncommercial-No Derivative Works 3.0 License](#).  
Copyright © 2011 Kristin Bush

LOYOLA UNIVERSITY CHICAGO

ROLE FOR HISTONE DEACETYLASES IN GLUCOCORTICOID RECEPTOR  
MEDIATED TRANSCRIPTION OF NATURAL KILLER CELL ACTIVITY

A THESIS SUBMITTED TO  
THE FACULTY OF THE GRADUATE SCHOOL  
IN CANDIDACY FOR THE DEGREE OF  
MASTER OF SCIENCE

PROGRAM IN MICROBIOLOGY AND IMMUNOLOGY

BY  
KRISTIN A. BUSH  
CHICAGO, IL  
DECEMBER 2011

COPYRIGHT BY KRISTIN A. BUSH, 2011  
All rights reserved

## ACKNOWLEDGEMENTS

I would like to thank Dr. Herbert Mathews, PhD, and Dr. Linda Witek-Janusek, for the guidance and support they provided from the moment I joined their lab and especially throughout the process of obtaining this degree. The unwavering confidence Dr. Mathews had in my abilities and ideas was invaluable to me during my graduate school career. Additionally, I would like to thank my lab mates, Justin Eddy, Karen Krukowski, Kelly Loster-Kosik, and Teresa Konley, who were always ready with suggestions and help to improve and assist my work.

I would like to thank the members of my thesis committee for their enthusiasm and encouragement of my work, as well as for their patience throughout the process.

Finally, I would like to thank all the members of my family, specifically my parents, who have encouraged me throughout my life and especially during the stress-filled experience of graduate school. Most of all, I thank my husband, Christopher, for the unwavering support and reassurance he offered each and every day.

## TABLE OF CONTENTS

ACKNOWLEDGEMENTS	iii
LIST OF FIGURES	vi
LIST OF ABBREVIATIONS	vii
ABSTRACT	ix
CHAPTER ONE: Introduction	1
CHAPTER TWO: Review of Literature	3
Breast Cancer and the Psychological Response	3
Stress and the Hypothalamic-Pituitary-Adrenal Axis	3
Glucocorticoids	5
Glucocorticoid Receptor	5
<i>Gene expression</i>	5
<i>Protein domains</i>	7
<i>Activation and Activity</i>	7
<i>Regulation</i>	8
Histone Deacetylases (HDACs)	10
<i>Class I HDACs</i>	11
<i>Classes 2, 3, and 4 HDACs</i>	12
Coregulator Complexes	13
<i>Corepressor Complexes</i>	13
<i>Nuclear Corepressor Complex and Silencing Mediator of Retinoid and Thyroid Hormone</i>	15
<i>Receptors</i>	15
The Epigenetic Code	17
Relevance to This Work	19
CHAPTER THREE: Hypothesis and Aim	20
CHAPTER FOUR: Materials and Methods	23
Cell Lines	23
Culture Conditions	23
Glucocorticoid Treatment	24
Natural Killer Cell Activity Assay	24
<i>Preparation of Cells</i>	24
<i>Natural Killer Cell Activity Assay</i>	25

Nuclear and Cytoplasmic Separation	26
Preparation of Whole Cells	27
Lysis of Whole Cells and Nuclei	27
Co-immunoprecipitation	27
<i>Lysate pre-clearing</i>	27
<i>Cross-linking antibody to magnetic beads</i>	28
<i>Co-Immunoprecipitation</i>	29
Western Blot	30
<i>Sample preparation</i>	30
<i>Gel electrophoresis and transfer</i>	30
<i>Immunoblotting</i>	30
<i>Quantification of Western Blot</i>	31
Statistical Analysis	31
Buffers and Solutions	32
CHAPTER FIVE: Results	34
Comparative analysis of natural killer cell activity of the YT-Indy cell line with and without dexamethasone treatment	34
Comparative analysis of the subcellular localization of the glucocorticoid receptor during dexamethasone treatment	36
Comparative analysis of the subcellular localization of HDACs 1, 2, and 3 during dexamethasone treatment	38
<i>HDAC1</i>	38
<i>HDAC2</i>	40
<i>HDAC3</i>	42
Interactions between GR, HDACs, and Corepressor Complexes	44
CHAPTER SIX: Discussion	48
APPENDIX A: Supplemental Figures	56
Supplemental Figure 1: Acetylation of H4-K8 during dexamethasone treatment	57
BIBLIOGRAPHY	58
VITA	67

## LIST OF FIGURES

Figure	Page
1. Hypothalamic-pituitary-adrenal axis	4
2. Glucocorticoid receptor domains	6
3. GR signal transduction pathway	9
4. NCoR and SMRT corepressor complexes	14
5. The domain structure of NCoR and SMRT	16
6. Formation of heterochromatin and euchromatin	18
7. NKCA	35
8. Subcellular localization of GR	37
9. Subcellular localization of HDAC1	39
10. Subcellular localization of HDAC2	41
11. Subcellular localization of HDAC3	43
12. Co-immunoprecipitation of Whole Cell Lysates	45
13. Co-immunoprecipitation of Nuclear Lysates	47

## LIST OF ABBREVIATIONS

Ab	antibody
ACTH	adrenocorticotrophic hormone
AF	activation function domain
CBP	cyclic AMP response element binding protein
CoREST	corepressor for RE1 silencing transcription factor
CRH	corticotrophin-releasing hormone
CTD	C-terminal domain
DBD	DNA-binding domain
Dex	dexamethasone
DMP	disintegrations per minute
EDTA	ethylenediamine-tetracetic acid
GC	glucocorticoid
GR	glucocorticoid receptor
GRE	glucocorticoid response element
H4K8	histone-4 lysine-8
HAT	histone acetyltransferase
HDAC	histone deacetylase
hGR	human glucocorticoid receptor
HPA	hypothalamic-pituitary-adrenal axis
HRP	horseradish peroxidase
HSP	heat shock protein



ID	interacting domains
IF	interferon
IL	interleukin
IP	immunoprecipitation
LBD	ligand binding domain
LU	lytic units
NAD	nicotinamide adenine dinucleotide
NCoR	nuclear receptor corepressor
NES	nuclear export signal
nGRE	negative glucocorticoid response element
NK	natural killer
NKCA	natural killer cell activity assay
NLS	nuclear localization sequence
NRS	nuclear retention signal
NTD	N-terminal domain
NURD	nuclear remodeling and histone deacetylation complex
PAGE	polyacrylamide gel electrophoresis
PBS	phosphate buffered saline
PER	perforin
RD	repressing domains
SDS	sodium dodecyl sulfate
SMRT	silencing mediator of retinoid and thyroid hormone
TBST	tris-buffered saline with tween
TNF	tumor necrosis factor
TSA	trichostatin A
WB	western blot

## **ABSTRACT**

During periods of psychosocial distress glucocorticoids (GCs) are known to reduce the lytic activity of natural killer cells (NKCA). Glucocorticoid treatment also reduces acetylation of histone residues; however, the glucocorticoid receptor (GR) lacks deacetylase activity. GR is known to interact with histone deacetylases (HDACs) and with corepressors that mediate gene transrepression. In this investigation, GC induced histone deacetylation was demonstrated to be due to GR recruitment of HDAC1 and the corepressor complex SMRT. These data show that reduced acetylation of immune functional genes associated with NKCA is likely due to histone deacetylation by HDAC1 and transrepression of those genes by SMRT.

## CHAPTER ONE

### INTRODUCTION

Diagnosis of breast cancer increases emotional distress<sup>1,2</sup>. Such psychological stress is associated with immune dysregulation<sup>1,3,4</sup>; in particular reductions in natural killer cell function are observed<sup>3</sup>. Psychological stress activates the hypothalamic-pituitary-adrenal axis (HPA), resulting in the secretion of glucocorticoids (GCs). Glucocorticoids, including cortisol, suppress immune function<sup>5,6</sup>.

Glucocorticoids enter the cell, bind to the glucocorticoid receptor (GR) in the cytoplasm, and the GR-GC complex translocates into the nucleus. Within the nucleus, GR inhibits transcription, which results in repression of associated genes<sup>7,8</sup>. GC treatment of a natural killer (NK) cell line (NK-92) corresponds with decreased global histone acetylation of residues H4-K8 and H4-K12, as well as reduced interferon- $\gamma$  and perforin levels and NK cell activity (NKCA)<sup>9</sup>. The molecular mechanism by which glucocorticoid treatment results in histone deacetylation is unknown.

GC treatment is associated with deacetylation of lysine residues on histone proteins; yet, GR lacks deacetylase activity<sup>10</sup>. GR is known to bind nuclear corepressor complexes that recruit histone deacetylases (HDACs)<sup>10</sup>. Therefore, it was hypothesized that GC treatment-induced histone deacetylation is due to GR recruitment of HDACs via corepressor complexes. This study

used a NK-like cell line (YT-Indy) and a synthetic glucocorticoid analog (Dexamethasone) to model the effect of GCs have on NK cells, in order to determine whether glucocorticoid receptor recruits HDACs as well as corepressor molecules, and if this reduces NK cell activity.

## **CHAPTER TWO**

### **REVIEW OF LITERATURE**

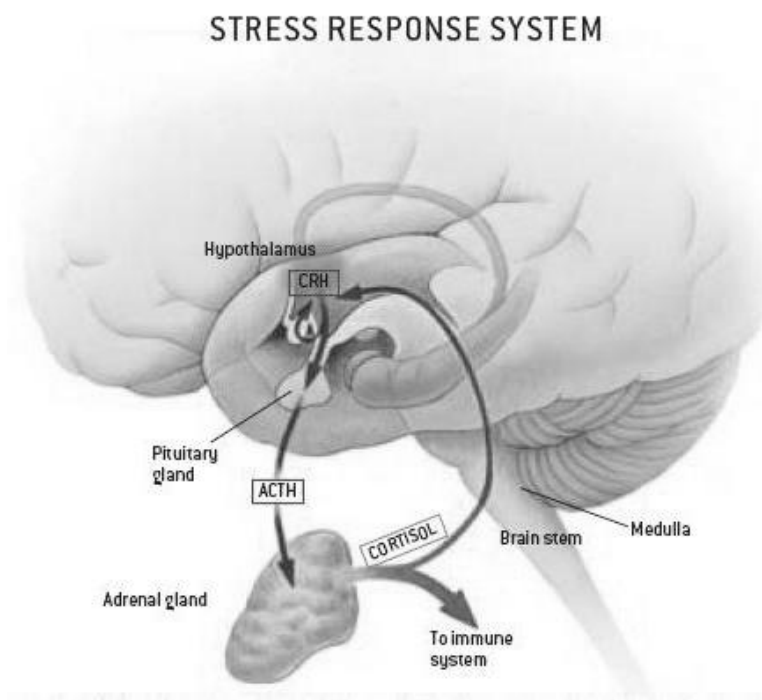
#### **2.1 Breast Cancer and Psychological Response**

Breast cancer is the second leading cause of death in American women<sup>11</sup>. Women diagnosed with breast cancer report heightened stress perception, anxiety, fear, uncertainty, and mood disturbance<sup>12-18</sup>. Psychological distress activates neuroendocrine pathways that increase levels of cortisol<sup>19,20</sup>, which impact immune function<sup>6</sup>.

#### **2.2 Stress and the Hypothalamic-Pituitary-Adrenal Axis**

Perceived stress activates the hypothalamic-pituitary-adrenal (HPA) axis (as depicted in figure 1), which leads to an increase in secretion of cortisol. The hypothalamus releases corticotrophin-releasing hormone (CRH), which stimulates the pituitary to release adrenocorticotropic hormone (ACTH). Within the adrenal gland, ACTH induces the synthesis and secretion of cortisol. Acute stress activates the HPA axis, elevating the levels of cortisol. Acute stress initially activates HPA and, as the stressor persists, HPA activation diminishes and cortisol levels decline<sup>21-25</sup>. Cortisol is elevated in women at breast cancer diagnosis<sup>1,4</sup>.

## Hypothalamic-Pituitary-Adrenal Axis



From: Eisen, 2011.

Figure 1. The HPA axis. Perceived stress activates the hypothalamus to release corticotrophin-releasing hormone (CRH). CRH induces the pituitary gland to release adrenocorticotrophic hormone (ACTH), which stimulates the adrenal gland to produce cortisol. Upon entry into the blood, cortisol encounters blood cells, including immune cells.

## 2.3 Glucocorticoids

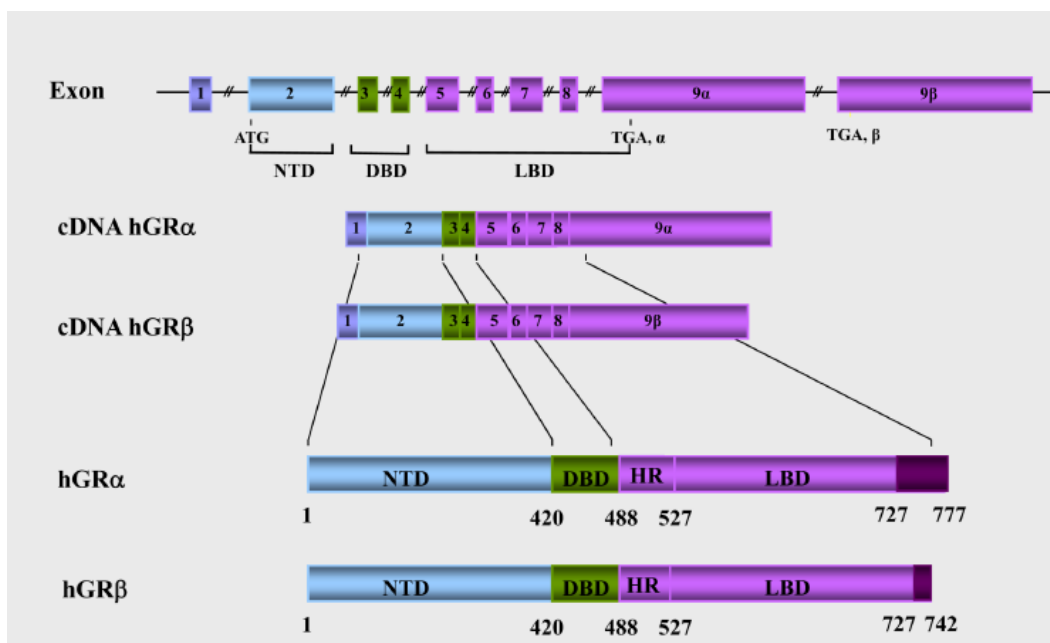
Glucocorticoids (GCs) regulate a variety of physiological functions, in addition to maintaining stress-related homeostasis<sup>27</sup>. Glucocorticoids are also widely prescribed as therapeutic treatments for inflammation, autoimmunity, and lymphoproliferative disorders<sup>28</sup>; however, long-term use is associated with various side effects and GC resistance. Cortisol, the most abundant glucocorticoid in humans, is produced by the adrenal gland; it is transported through the blood bound to corticosteroid-binding globulin (CBG) and albumin<sup>29</sup>. Cortisol, like other steroid-derived lipophilic ligands, diffuses through the cell membrane into the cytoplasm, where it binds and activates its cognate receptor<sup>30</sup>.

## 2.4 Glucocorticoid Receptor

### A. Gene expression

Glucocorticoid receptor (GR) is a member of the nuclear receptor super family, and is encoded by the gene *nr3c1* on human chromosome 5 (region 5q31p). The human GR (hGR) gene consists of nine exons; alternative splicing of exon 9 results in two highly homologous protein forms,  $\alpha$  and  $\beta$ . The hGR $\alpha$  functions as a ligand-dependent transcription factor when activated, and is expressed in most tissues. The hGR $\beta$  does not bind glucocorticoid agonists, and is not as ubiquitously expressed as hGR $\alpha$ ; hGR $\beta$  acts as a dominant-negative, suppressing GR $\alpha$ 's activity<sup>10</sup>. In addition to alternative splicing, multiple isoforms of hGR $\alpha$  are created by using the 8 alternative translation initiation sites; *nr3c1* has three different promoters as well.

## Glucocorticoid Receptor Domains



From: Nicolaidis, et al., 2010.

Figure 2. The structure of the human glucocorticoid receptor gene (nr3c1). hGR consists of 9 exons; alternative splicing of exon 9 results in two isoforms, hGR $\alpha$  and hGR $\beta$ . The N-terminal domain (NTD), depicted in light blue, contains the major transactivation domain. Adjacent to the NTD, the DNA-binding domain (DBD) contains sequences for binding to GREs, dimerization, and nuclear translocation; it is shown in green. The hinge region (HR) is between the DBD and the ligand-binding domain (LBD), which is the site of glucocorticoid binding.



### *B. Protein domains (figure 2)*

GR's N-terminal domain (NTD) contains the major transactivation domain, known as activation function (AF)-1, which is ligand-independent. This domain is involved in initiation of transcription. GR's DNA-binding domain (DBD) is located adjacent to the NTD; it has two zinc finger motifs that bind to specific DNA sequences known as glucocorticoid response elements (GREs). The DBD also contains sequences important for receptor dimerization and nuclear translocation. The hinge region is between the DBD and the ligand-binding domain (LBD), which forms the C-terminus of GR. The LBD binds glucocorticoids and plays a critical role in ligand-induced activation of the receptor. The LBD also contains a second transactivation domain (AF-2), which is ligand-dependent, and is involved in dimerization, nuclear translocation, binding to heat shock proteins, and interaction with coactivators<sup>10</sup>. Most of the variability between isoforms is present in the NTD or CTD; the DBD remains constant<sup>10</sup>.

### *C. Activation and Activity*

In the unactivated state, hGR exists predominantly within the cytoplasm, bound to a multimeric molecular chaperone complex, which includes heat shock proteins (HSPs) 90, 70, and 50, and immunophilins. HSP90 regulates ligand binding, retains GR in the cytoplasm, and masks GR's two nuclear localization sequences (NLS); NL1 and NL2, which are adjacent to the DBD and in the LBD, respectively. Upon binding ligand (glucocorticoids), GR undergoes conformational changes that releases it from chaperone proteins and reveal GR's NLS, inducing rapid transit into the nucleus. Although uninduced GR is predominantly cytoplasmic and activated GR is

predominantly nuclear, both activated and unactivated GR forms have been shown to shuttle between the nucleus and cytoplasm depending on both the NLS and the nuclear retention signal (NRS)<sup>10</sup>.

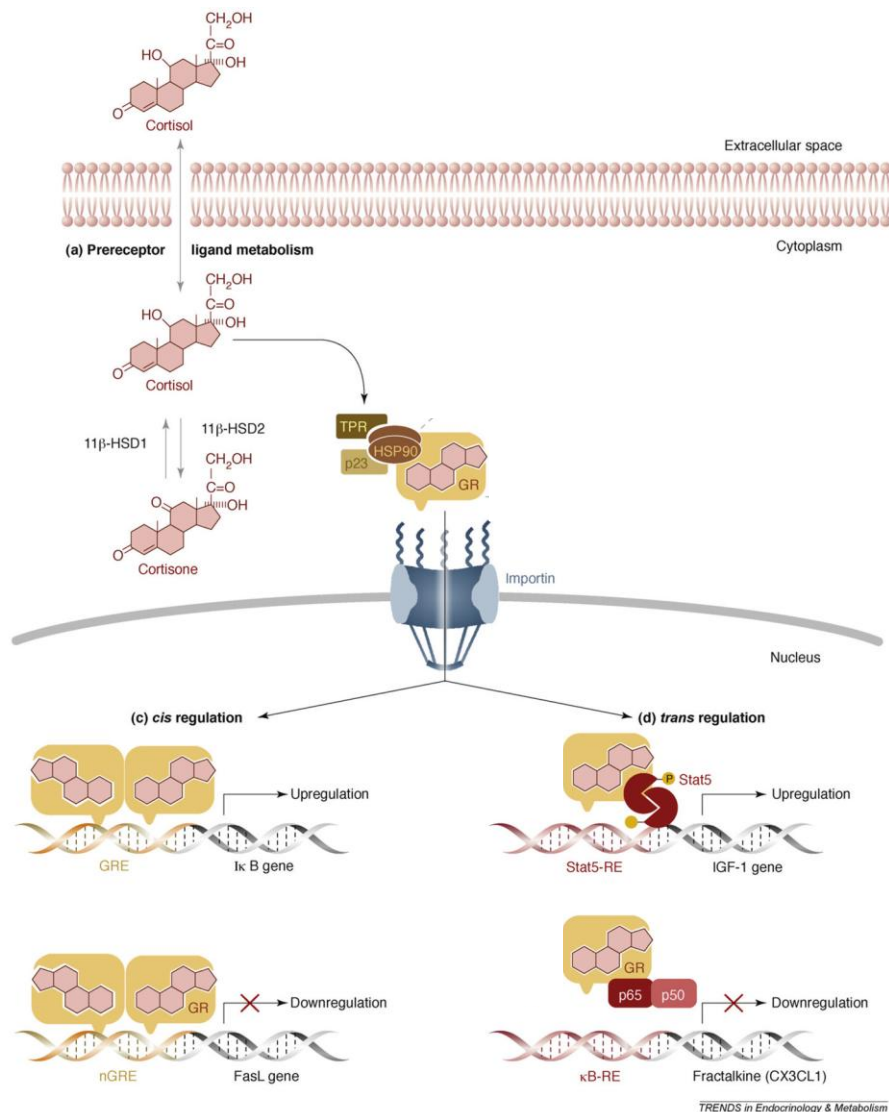
Once in the nucleus, the activated GR-corticosteroid complexes can homodimerize via their zinc finger DBDs, and bind to GREs in promoter regions of corticosteroid-responsive genes (figure 3). GR binding to GREs increases gene transcription via *cis*-activation<sup>31</sup>. However, negative GRE sites, in which GR binds a GRE and, through *cis*-repression, suppresses gene transcription, have also been identified<sup>32</sup>.

In addition to interaction with DNA directly, activated GR is also known to interact with other transcription factors through protein-protein interactions. Many inflammatory genes lack GRE sites, but are transcriptionally repressed by glucocorticoids<sup>33</sup>. The anti-inflammatory effects of GCs are mediated through *trans* repression (figure 3), as GR interacts and interferes with the transcription factors AP-1 and NF- $\kappa$ B<sup>34,32</sup>. GCs inhibit histone H4K8 and K12 acetylation by reducing the histone acetyltransferase (HAT) activity of cyclic AMP response element binding protein (CBP). Additionally, GC administration can increase histone deacetylase 2 (HDAC2) expression and target HDAC2 to NF- $\kappa$ B CBP complexes, which is associated with halted transcription of NF- $\kappa$ B-dependent genes<sup>35-37</sup>.

#### *D. Regulation*

The glucocorticoid receptor is regulated at multiple levels. First, basal expression of GR mRNA is controlled by the transcription factors c-Myb and Ets<sup>38</sup>. However, glucocorticoids

## GR Signal Transduction Pathway



From Gross and Cidlowski, 2008.

Figure 3. Activation and activity of GR. Cortisol enters the cell, dissociates GR from its chaperone protein complex, and induces translocation into the nucleus. Within the nucleus, GR dimers bind to DNA directly at GREs; this *cis* regulation can either upregulate or downregulate gene expression. GR can also interact with transcription factors through protein-protein interactions to up- or down-regulate transcription *in trans*. In the case of STAT proteins, STAT-5 as an example (d), GR interacts with DNA-bound STAT proteins to coactivate transcription from the STAT response element.

negatively regulate GR mRNA expression, as GR's promoter contains a negative glucocorticoid response element (nGRE), to which liganded GR binds and represses transcription. GR's promoter has NF- $\kappa$ B, AP-1, and CREB regulatory motifs, which are sites for binding of these transcription factors that positively regulate GR transcription. Liganded GR is known to repress the transcriptional activity of NF- $\kappa$ B and AP-1 by preventing interaction with transcription factors, coactivators or the DNA, itself<sup>37</sup>. In addition to transcriptional regulation, GR undergoes several post-translational modifications, including phosphorylation, acetylation, sumoylation, and ubiquitination before and after ligand binding. These modifications can influence subcellular trafficking, cofactor interaction, transcriptional activation, receptor stability, and turnover<sup>30</sup>.

Unactivated GR predominantly exists within the cytoplasm, while activated GR is mostly nuclear. Constitutive shuttling between these compartments occurs for both the activated and inactive forms of GR<sup>40</sup>. GR's subcellular location at any given time is determined by the accessibility of GR's two NLSs to nuclear import protein<sup>41,42</sup>, the availability and accessibility of nuclear export proteins<sup>43</sup>, and the exposure of GR's nuclear retention signal (NRS)<sup>44</sup>.

In addition to regulating expression and localization, exposure to glucocorticoids decreases the level of GR by degradation through the proteasome-ubiquitin pathway<sup>45</sup>.

## **2.5 Histone Deacetylases**

Histone deacetylases (HDACs) are enzymes that remove acetyl groups from the  $\epsilon$ -amino group of lysines on the N-terminal tails of histone proteins. In general, increased levels of histone acetylation (hyperacetylation) are associated with increased transcription, while decreased acetylation (hypoacetylation) is associated with transcriptional repression. Currently, eighteen HDACs have been identified; they are divided into four classes based on their homology with yeast

orthologs. All HDACs, except class III, contain a conserved catalytic domain that uses a charge relay system to remove acetyl groups from target lysine residues;  $Zn^{2+}$  ion must be present within the zinc binding site of the catalytic pocket during the reaction. HDACs also deacetylate other cellular proteins, including p53, E2F,  $\alpha$ -tubulin, and MyoD<sup>46,47</sup>.

#### A. Class I HDACs

Class I HDACs include HDAC 1, 2, 3, and 8, which contain a well-conserved catalytic domain and are related to the *S. cerevisiae* HDAC Rpd3. The catalytic domain of Class I HDACs is located at the N-terminus, and comprises the majority of the protein<sup>48</sup>. The distinguishing features of class I HDACs are the C-terminal domains, which are more divergent<sup>49</sup>.

HDACs 1 and 2 are most closely related, having 82% sequence homology, while HDACs 3 and 8 are most closely related to each other, sharing 34% homology. HDACs 1, 2, and 3 are known to associate with multiprotein complexes. Both HDAC 1 and 2 are only active when complexed with mSin3A, nucleosome remodeling and histone deacetylation (NURD), or corepressor for RE1 silencing transcription factor (CoREST) corepressor complexes; silencing mediator of retinoic acid and thyroid hormone (SMRT) and nuclear receptor corepressor (NCoR) complexes are required for HDAC3's activity<sup>50</sup>, although HDACs 1 and 2 are also known to associate with both SMRT and NCoR<sup>51-55</sup>. Additionally, both HDAC1 and HDAC2 have been shown to be recruited by GR<sup>56,35</sup>. Like other class I HDACs, HDAC8 is ubiquitously expressed; however, HDAC8's activity has been mostly limited to smooth muscle<sup>57</sup>.

HDACs 1 and 2 are predominantly located in the nucleus, while HDAC3 is found in the nucleus, the cytoplasm, and is sometimes associated with the plasma membrane<sup>58</sup>. Class I HDACs contain an NLS; however, only HDAC3 has a nuclear export signal (NES)<sup>59</sup>. HDAC1 requires a shuttle protein for nuclear export.

#### *B. Classes II, III, and IV HDACs*

Class II HDACs are evolutionarily related to class I HDACs, and have the same catalytic activity. Class II is homologous to yeast protein HDA1. While class I is ubiquitously expressed in most tissues, class II HDAC are expressed mostly in heart, brain, lung, spleen, kidney and smooth muscle<sup>59</sup>. Although class II HDACs can associate with protein complexes, such an association is not required for enzymatic activity. Class II HDACs are also stimulated to shuttle between the cytoplasm and nucleus<sup>60</sup>; this activity is often regulated by phosphorylation status of the HDACs.

Class III HDACs are evolutionarily unrelated to any other class of HDACs; they catalyze the transfer of acetyl groups to NAD, which is a required cofactor for class III activity. The difference in catalytic activity protects class III HDACs from the effect of HDAC inhibitors, e.g. TSA and vorinostat. Class III HDACs are known as sirtuins, as they share homology with yeast Sir2. Sirt1 and Sirt2 shuttle between the nucleus and cytoplasm<sup>83</sup>. Sirt6 and Sirt7 are found in the nucleus, and Sirt3, -4, and -5 are found in mitochondria<sup>83</sup>. Class III HDACs are expressed in brain, heart, kidney, liver, pancreas, spleen, adipose, skeletal muscle, and nervous system tissues<sup>83</sup>.

Class IV HDACs, of which HDAC11 is the only member, are phylogenetically unrelated to class I or class II, yet share sequence homology within the catalytic site with classes I and II<sup>61</sup>.

HDAC11 shuttles between the nucleus and cytoplasm, and is expressed only in certain tissues, including the heart, brain, kidneys, and skeletal muscle<sup>62</sup>. HDAC11's regulatory role is still undetermined.

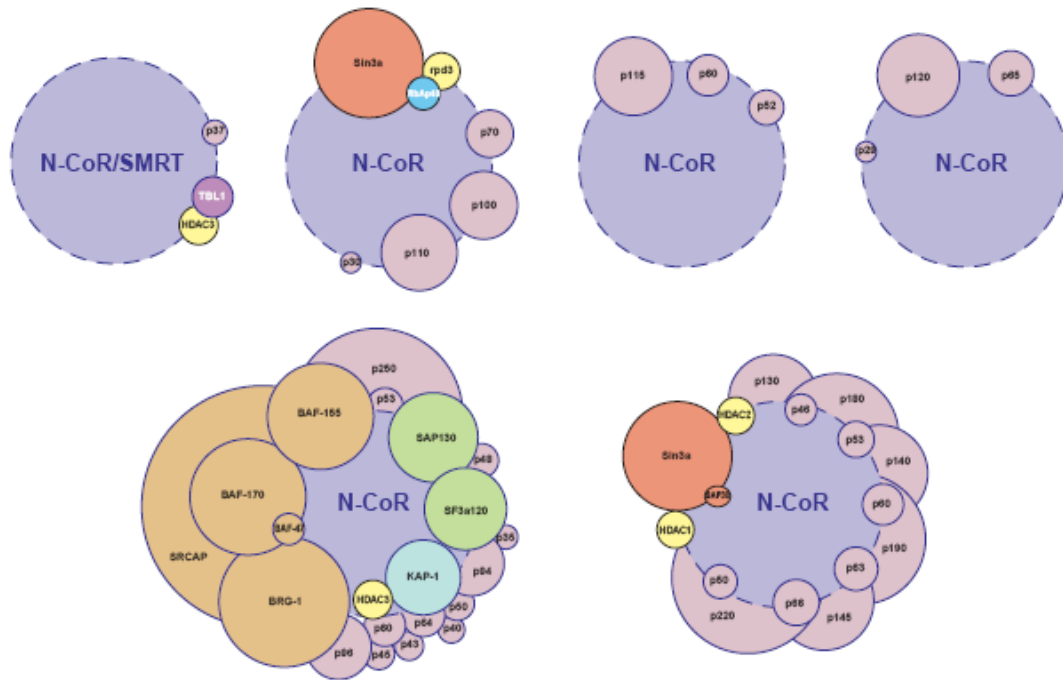
## 2.6 Coregulator Complexes

Gene regulation is controlled in a number of ways, one of which is by enzymatic complexes that are known as coactivators and corepressors. These “sense” and integrate cellular signals and can mediate chromatin modifications that impact transcription. Coregulator complexes are composed of many subunits, and can be divided into two generic classes based on enzymatic activity: those that are capable of modifying histone tails and those that are ATP-dependent and serve to remodel chromatin. The latter group presumably acts by modifying the interface between histone proteins and DNA itself; this activity results in nucleosomal sliding<sup>63</sup>. Enzymes capable of covalently modifying histone tails include HDACs, histone acetyltransferases (HATs), methyltransferases, demethylases, kinases, phosphatases, ubiquitinases, and SUMO ligases.

### A. Corepressor Complexes

Corepressor complexes are composed of several factors that “act in a combinatorial manner to antagonize the actions of coactivator complexes . . . and by mediating covalent modifications . . . that serve as marks for recruitment of additional factors involved in transcriptional repression,” (Rosenfeld, 2006). Corepressor complexes (figure 4) include the nuclear corepressor complex (NCoR), the silencing mediator of retinoid and th thyroid hormone receptors (SMRT), the

### NCoR and SMRT corepressor complexes



From Jepsen and Rosenfield, 2002.

Figure 4. Corepressor complexes that include NCoR and SMRT. Each complex contains a core protein, either NCoR or SMRT. Other proteins, including HDACs, and even other protein complexes, for example Sin3a, interact with the core protein to form a large corepressor complex. The association of various components consolidates a variety of repressive functions, including histone deacetylation, ATP-dependent chromatin remodeling activity, and DNA methylation, into a single complex.

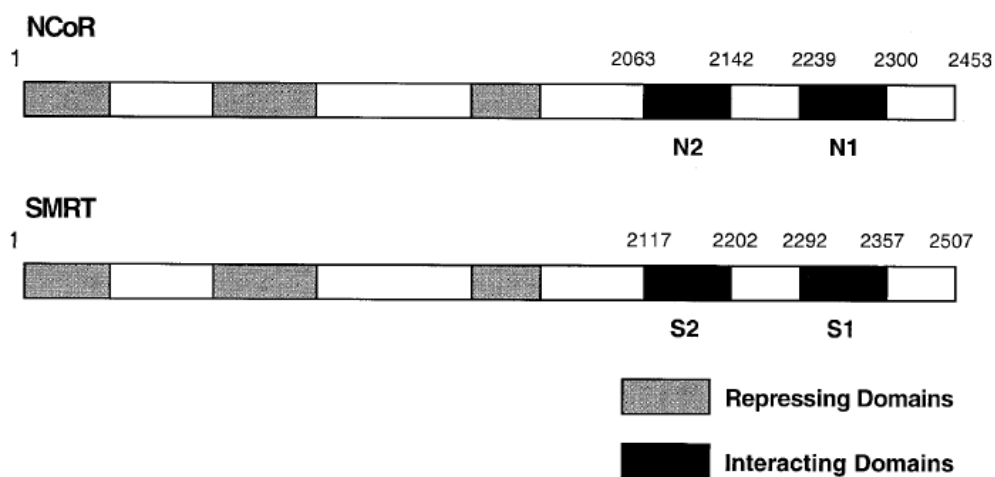


sin3-sin associated protein complex (Sin3-SAP), the nucleosome remodeling and histone deacetylation complex (NURD), the NURD-related HDAC-complex, and the CoREST –HDAC complex. These related complexes are composed of a core protein that has sites for interaction with various cofactors, which depend on the activation status of the cofactors. Cell-signaling events also impact the composition of proteins in corepressor complexes<sup>64</sup>.

#### *B. Nuclear Receptor Corepressor Complex and Silencing Mediator of Retinoid and Thyroid Hormone Receptors*

NCoR and SMRT are two of the many nuclear corepressor proteins, which recruit multiprotein complexes with histone deacetylase activity. This results in chromatin modification, preventing transcription. As figure 5 depicts, both NCoR and SMRT are modular proteins that have at least three repressing domains (RDs) in their NTDs, and two interacting domains (IDs) in their CTDs. The IDs mediate interaction with nuclear receptors; although the IDs of NCoR and SMRT share structural similarities, the amino acid sequences of IDs between proteins are only 23% to 53% homologous. These differences in sequence homology suggest that NCoR and SMRT interact with nuclear receptors differently, and may possibly determine recruitment specificity in that each corepressor has nuclear receptors<sup>66</sup>. Certain nuclear receptors are only able to interact with one of these corepressors, for example, the receptor RevErb only associates with NCoR<sup>67</sup>. Other nuclear receptors are capable of interacting with either corepressor, but preferentially recruit one complex over others<sup>64</sup>.

### The domain structure of NCoR and SMRT



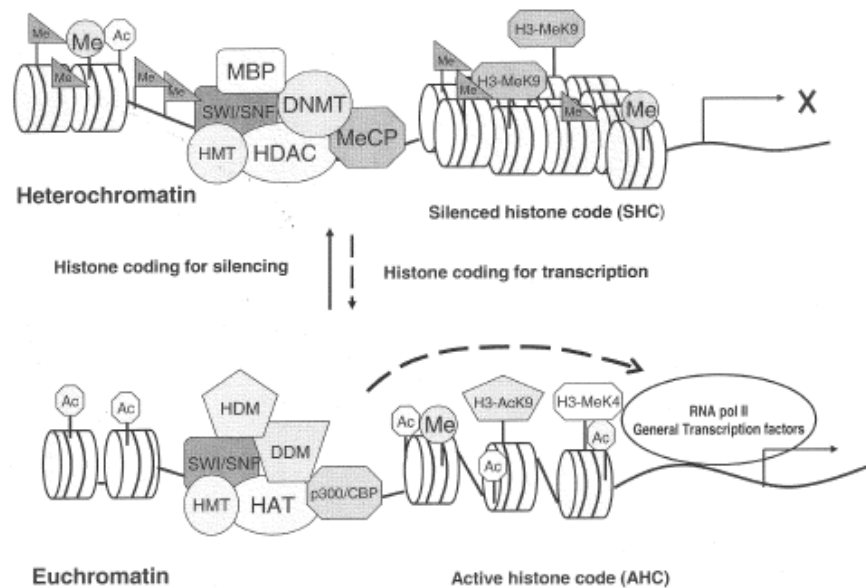
From: Cohen, et al., 2000.

Figure 5. The domain structure of NCoR and SMRT. Three repression domains (in grey) are present in the N-terminus of the protein. HDACs can interact with NCoR or SMRT through sequences within and adjacent to the repression. The interaction domains (in black) are located at the C-terminus; these allow for interaction with nuclear receptors and other transcription factors. It is the interacting domains of NCoR and SMRT that are distinct, resulting in specific preferences for members of the nuclear receptor family.

## 2.7 The Epigenetic Code

Epigenetic regulation is mediated by covalent modifications that impact gene expression without altering the DNA sequence<sup>84</sup>. These processes can result in heritable changes in gene expression or in stable, long-term alterations of the transcriptional potential of the cell, which may not be heritable. DNA is wrapped around an octomeric protein complex, consisting of two of each of the histone proteins (H2A, H2B, H3, and H4). The combination of 146 bps of DNA and histone proteins composes the nucleosome, the basic unit of chromatin. Epigenetic changes include either DNA methylation, which affects the accessibility of DNA, or modifications of N-terminal tails of histone proteins that indirectly impact DNA accessibility due to compaction or relaxation of chromatin structure<sup>85,86,87</sup> (figure 6). Modifications of residues on histones include acetylation<sup>88</sup>, deimination<sup>89</sup>, methylation<sup>90</sup>, phosphorylation<sup>91</sup>, proline isomerization<sup>92</sup>, sumoylation<sup>93</sup>, and ubiquitination<sup>94</sup>. Acetyl groups are added to lysine residues, neutralizing their positive charge, disrupting the interaction with DNA's negative charge, and loosening the compaction of chromatin<sup>95</sup>. Relaxing the chromatin structure increases its accessibility to transcription factors and, subsequently, gene expression. Removal of acetyl groups results in condensation of chromatin, repressing gene expression<sup>95</sup>.

## The epigenome, histone modifications, and transcription



From Thiagalingam et al., 2003.

Figure 6. Formation of heterochromatin and euchromatin. Corepressor complexes, containing HDACs to remove acetyl groups and DNA methyltransferases (DNMT) to methylate lysines, modifying histone tails to form heterochromatin, which silences transcription. Coactivator complexes, including histone acetyltransferases (HAT) acetyl lysines and DNA demethylases (DDM), which remove methyl groups, relax chromatin to allow for gene transcription.

## 2.8 Relevance to this work

As previously discussed, the emotional distress brought on by breast cancer diagnosis is known to result in immune dysregulation<sup>1-4</sup>, specifically reductions in NK cell activity<sup>3</sup>. As psychosocial stress activates the HPA to release cortisol *in vivo*, the effects of a GC was modeled *in vitro* with the synthetic GC, dexamethasone. Previous work from this laboratory has demonstrated that decreased NK cell activity was due to decreased expression of immune relevant genes, including perforin and interferon- $\gamma$ <sup>9</sup>. Reduced expression of those proteins was associated with reduced acetylation of histone residues within the promoter regions of those genes. Reduced acetylation results in chromatin compaction and reduced accessibility of those promoter regions to transcriptional machinery<sup>95</sup>. The specific molecules mediating histone deacetylation during glucocorticoid treatment are unknown.

Glucocorticoid treatment is known to activate the glucocorticoid receptor, which is a nuclear receptor known to impact transcription. However, GR lacks deacetylase activity itself, but it is known to interact with many of the nuclear corepressor complexes, which recruit histone deacetylases. Thus, this project will evaluate whether histone deacetylation during GC treatment is a result of GC-activated GR binding of a corepressor complex, NCoR or SMRT, which may recruit HDAC 1, 2, or 3.

## CHAPTER THREE

### HYPOTHESIS AND AIM

The immunosuppressive effects of glucocorticoids (GCs) are well documented<sup>5,6,69,70</sup>. In particular, reductions in natural killer (NK) cell activity<sup>9,72,73</sup> and reduced production of effector molecules, including perforin, and inflammatory cytokines, specifically IFN- $\gamma$  and IL-6<sup>9</sup>, result from GC treatment. Diminished production of immune molecules is due to decreased transcription of the genes, which is caused by decreased acetylation of lysine residues on histone tails. Removal of acetyl groups results in compaction of the chromatin structure creating promoters that are inaccessible to transcription factors<sup>95</sup>. Although decreased histone acetylation is observed during GC treatment, the molecular mechanism by which glucocorticoids affect acetylation is unknown. However, acetylation status, transcript and protein levels of effector molecules and cytokines, as well as NK cell function are restored when GC-treated cells are exposed to a histone deacetylase (HDAC) inhibitor<sup>9</sup>. Therefore, it is probable that glucocorticoids induce HDACs, which deacetylate histone tails.

Glucocorticoids diffuse through the cell membrane, dissociate glucocorticoid receptor (GR) from its cytoplasmic chaperone proteins, and induce translocation of GR into the nucleus. Within the nucleus, GR can activate or repress transcription through direct or indirect interactions with DNA. GCs are known to suppress inflammatory gene expression, specifically those regulated by

NF- $\kappa$ B and AP-1. Many inflammatory gene promoters lack glucocorticoid response elements<sup>33</sup>, suggesting that GR-mediated suppression occurs without GR binding to DNA. GR is known to bind both NF- $\kappa$ B and AP-1 and inhibit transcription of NF- $\kappa$ B and AP-1-regulated inflammatory genes<sup>34,32</sup>. The promoter regions of such genes have reduced histone acetylation during GC treatment<sup>9</sup>. However, GR itself lacks deacetylase activity<sup>10</sup>. GR is known to interact with nuclear corepressor complexes<sup>30</sup>, which recruit HDACs<sup>50</sup>. Thus, it is **hypothesized** that the glucocorticoid receptor interacts with HDACs during glucocorticoid treatment. It is probable that GR's recruitment of HDACs mediates the deacetylation of histone tails that GCs are known to induce.

The **aim** of this project was to determine if GR, when bound by GC, recruits HDACs. To assess recruitment of HDACs by, a model system using a natural killer-like cell line (YT-Indy) and a synthetic glucocorticoid analogue (Dexamethasone) was employed. Dexamethasone (Dex) has been demonstrated to both reduce acetylation of histone 4-lysine 8 (H4K8) residue (Krukowski, unpublished data; supplemental figure 1) and decrease the lytic activity of YT-Indy cells (Bush, unpublished data, figure 7). Since Dex decreases NK cell activity and also reduces histone acetylation in the YT-Indy cell line, (which expresses both GR and HDACs,) this cell line was used to evaluate the interactions among GR and HDACs.

There are eighteen HDACs, which are divided into four classes based on homology to yeast HDACs. Class I HDACs, including HDACs 1, 2, 3, and 8, are ubiquitously expressed in most tissues; although the activity of HDAC8 may be restricted to smooth muscle cells<sup>57</sup>. Additionally, class I HDACs are involved in epigenetic regulation, as transcriptional repressors<sup>61</sup>. HDACs 1, 2, and 3 require activation by nuclear corepressor complexes<sup>50</sup>, including nuclear receptor

corepressor (NCoR) and silencing mediator of retinoid and throid hormone (SMRT). Both NCoR and SMRT are known to repress genes regulated by NF- $\kappa$ B and AP-1, and are known to interact with nuclear receptors<sup>65</sup>. Therefore, interactions between GR and HDACs 1, 2, and 3 were assessed, as well as interactions between GR and NCoR and SMRT to address this aim.

YT-Indy cells were cultured in the presence or absence of Dex, and then subjected to co-immunoprecipitation assays targeting GR, HDACs 1, 2, or 3, NCoR, or SMRT. To determine if HDACs immunoprecipitated with GR, western blot analysis of co-immunoprecipitations was used.



## CHAPTER FOUR

### MATERIALS AND METHODS

#### 4.1 Cell Lines

YT-Indy, a natural killer-like cell line (from Christopher J. Froelich, M.D. Northwestern University) is a subline of YT, which was originally established from a child with acute lymphoma and thymoma<sup>74</sup>. YT cell lines are cytotoxic, respond to IL-2, but lack rearranged TCR- $\beta$  genes. YT-Indy cells are capable of killing target cells upon stimulation of the CD28 receptor by its ligand CD80/CD86 on the target cells<sup>75</sup>. Additionally, YT-Indy cells do not express killer inhibitory receptors (KIRs) or C-type lectins on the cell surface<sup>76</sup>. YT-Indy cells are IL-2 independent, and proliferate continuously *in vitro* without conditioned media.

K652, a human erthyleukemic-like cell line, was obtained from the American Type Culture Collection. K652 cells are highly sensitive targets of *in vitro* NK cell cytotoxicity.

#### 4.2 Culture Conditions

Both YT-Indy cells and K562 cells were maintained at 37°C in an atmosphere of 5% CO<sub>2</sub> in suspension cultures in 75 cm<sup>2</sup> tissue culture flasks (Corning Glass Works). The YT-Indy cell line was cultured in media containing RPMI 1640 (Invitrogen) at 2.5 x 10<sup>5</sup> cells/ml supplemented with

12% fetal bovine serum low LPS (Sigma), 100 units/ml penicillin (Invitrogen), 100 µg/ml streptomycin (Invitrogen), 0.1mM non-essential amino acids (Invitrogen), 0.1mM 2-mercaptoethanol (Invitrogen), and 2mM L-glutamine (Invitrogen). The K562 cell line was cultured in K562 media, composed of RPMI 1640 at  $2.5 \times 10^5$  cells/ml supplemented with 10% fetal bovine serum (FBS) low LPS, 100 units/ml penicillin, 100 µg/ml streptomycin, 0.1mM non-essential amino acids, 0.1mM 2-mercaptoethanol, and 2mM L-glutamine.

### **4.3 Glucocorticoid Treatment**

Dexamethasone (Dex) (Sigma), a synthetic glucocorticoid analogue, was used to simulate cortisol. YT Indy cells, cultured at  $2.5 \times 10^5$  cells/ml, were treated in 75 cm<sup>2</sup> tissue culture flasks with 100nM ( $10^{-7}$ M) Dex for 2, 4, 8, and 24 hours. This concentration of Dex did not decrease cell viability and is a concentration demonstrated previously to differentially regulate dexamethasone responsive genes<sup>77</sup>. After treatment with Dex, YT Indy cells were counted, and viability was assessed using 0.1% Trypan blue. Cells were resuspended to  $5 \times 10^6$  cells/ml in RPMI media lacking all supplements.

### **4.4 Natural Killer Cell Activity**

#### *A. Preparation of Cells*

K562 tumor cells were radioactively labeled with 100 µCi of [<sup>51</sup>Cr] (New England Nuclear). K562 cells were incubated at 37°C with [<sup>51</sup>Cr] in a 10ml conical tube for 1 hour, briefly shaking every 15 minutes to prevent cells from pelleting. After 1 hour incubation, cells were pelleted by centrifugation at 1,000 rpm for 3 minutes. The supernatant containing radioactivity was removed

using a glass pipette and discarded. The pelleted K562 cells were washed with 15 ml K562 media; cells were pelleted at 1,000 rpm for 10 minutes, and the wash media was discarded. The washing and pelleting steps were repeated three times. After washing, K562 cells were resuspended in 1 ml K562 media; cell number and viability were assessed using 0.1% Trypan blue.  $5 \times 10^5$  K562 cells were added to 10 ml K562 media, (resulting in a final concentration of  $5 \times 10^4$  cells/ml.)

Dex- and non-treated YT-Indy cells were collected from culture flasks in a 50ml conical tube, and pelleted at 1,000 rpm for 5 minutes. Cells were washed with PBS, and pelleted at 1,000 rpm for 5 minutes. Cells were resuspended with YT-Indy media, and counted using 0.1% Trypan blue. Cells were resuspended to a concentration of  $5 \times 10^6$  cells/ml.

#### *B. Natural Killer Cell Activity Assay*

YT -Indy cell lytic activity against tumor targets was assessed by chromium release assay as previously described<sup>1</sup>. One-hundred  $\mu$ l radiolabeled K562s were plated in a 96-well plate (Fisher). Dex- and non-treated YT-Indy cells were added to the wells to achieve effector to target ratios of 30:1, 20:1, and 10:1. Additional K562 media was added to bring the final volume to 200  $\mu$ l/well. Additionally, 6 wells of K562 cells were plated to determine the maximal and minimal radioactivity released by K562 cells. The NKCA plate was incubated for 4 hours at 37°C. After the incubation, supernatants were removed using a Skatron harvesting press and the associated radioactivity was determined. Results are expressed as percent cytotoxicity, calculated as: % Cytotoxicity = [(experimental DPM) – (minimum DPM)] / [(maximum DPM) – (minimum DPM)] x 100.

DMP is disintegrations per minute. All experimental means were calculated from triplicate values. Lytic units (LU) were calculated using a program written by David Coggins, FCRC, Frederick, MD. LU represents the number of cells per  $10^7$  effectors required to achieve 20% lysis of the target cells.

#### **4.5 Nuclear and cytoplasmic separation**

Dex- and non-treated YT-Indy cells were harvested from culture flasks, and pelleted at 1,000 rpm for 5 minutes. Cells were counted using 0.1% Trypan blue, and resuspended to  $5 \times 10^6$  cells/ml in YT-Indy media lacking supplements. Nuclear and cytoplasmic fractions of YT-Indy cells were separated using ProteoJET Cytoplasmic and Nuclear Protein Extraction Kit (Fermentas). Briefly, 1 ml of YT-Indy cells ( $5 \times 10^6$  cells) were placed in a microfuge tube; cells were pelleted 500 x g for 5 minutes. Pelleted cells were washed with 1 ml of phosphate buffered saline (PBS); cells were centrifuged 500 x g for 5 minutes, and supernatant was discarded. The pelleted cells were resuspended by adding 200  $\mu$ l of cell lysis buffer and vortexing the tube at low speed for 10 seconds. Tubes were incubated on ice for 8 minutes, and vortexing was repeated. To separate the cytoplasm from the nuclear fraction, tubes were centrifuged at 500 x g for 7 minutes at 4°C. The supernatant, which contained the cytoplasmic contents, was removed without disturbing the pellet and placed in another microcentrifuge tube and put on ice. The pelleted nuclei were resuspended by adding 500  $\mu$ l nuclei wash buffer, and vortexing until pellet disappeared. Tubes were incubated on ice for 2 minutes, and vortexing was repeated. Tubes were centrifuged for 7 minutes at 500 x g at 4°C. This washing step was repeated once. The pelleted nuclei were resuspended by adding 150  $\mu$ l ice cold nuclei storage buffer to each tube.

#### **4.5 Preparation of whole cells**

Dex- and non-treated YT-Indy cells were harvested from culture flasks, and pelleted at 1,000 rpm for 5 minutes. Cells were counted using 0.1% Trypan blue, and resuspended to  $5 \times 10^6$  cells/ml in YT-Indy media lacking supplements. 1 ml of YT-Indy cells ( $5 \times 10^6$  cells) was placed in a microfuge tube.

#### **4.6 Lysis of whole cells and nuclei**

Tubes containing whole cells and nuclei from the nuclear and cytoplasmic fraction steps were centrifuged for 5 minutes at 500 x g. The supernatants were discarded, and the pellets were resuspended with 1 ml ice cold PBS. Tubes were centrifuged for 5 minutes at 500 x g, and the supernatant was discarded. The pellet was resuspended with 500  $\mu$ l non-denaturing lysis buffer (20mM Tris HCl pH=8, 137 mM NaCl, 10% glycerol, 1 % Nonidet P-40, 2mM EDTA) and 2  $\mu$ l of protease inhibitor cocktail. Tubes were incubated for 30 minutes at 4°C with constant rotation using a GyroMini rotating platform (Dot Scientific). Tubes were centrifuged for 10 minutes at 10,000xg. The supernatant was aspirated from the pellet, and placed into a new microcentrifuge tube.

#### **4.7 Co-immunoprecipitation**

##### *A. Lysate preclearing*

To nuclear and whole cell lysates, 25  $\mu$ l of Protein G magnetic beads (New England BioLabs) was added. To tubes containing the cytoplasmic contents, 10  $\mu$ l of Protein G magnetic beads was added. Tubes were incubated for 1 hour at 4°C with constant rotation using a GyroMini

rotating platform. The beads were collected by magnetic separation, and the supernatant placed into a new tube. This step removes any cellular contents that would bind to the magnetic beads.

#### *B. Cross-linking antibody to magnetic beads*

The antibody used for immunoprecipitation was added to a tube containing borate buffer (0.2M boric acid, 50mM sodium tetraborate decahydrate, pH = 9.0). The antibodies used for immunoprecipitation were specific for GR (AbCam ab3671), HDAC1 (Millipore 06-720), HDAC2 (AbCam ab32117), HDAC3 (AbCam ab32369), NCoR (AbCam ab24552), SMRT (AbCam ab24551), and normal mouse IgG (Millipore 12-371). The dilution factors (antibody:precleared lysate) used for each antibody were as follows: 1:20 for GR and HDAC1, 1:60 for HDAC2, and 1:50 for HDAC3, NCoR, and SMRT. The proper volume of antibody was added to the borate buffer to achieve the optimal dilution for the antibody and to arrive at a volume of 500  $\mu$ l of antibody in borate buffer solution. The optimal dilutions were determined by testing a series of experimental dilutions, selecting the dilution that gives the strongest positive reaction with minimum background.

Fifty  $\mu$ l Protein G magnetic beads were placed into a microfuge tube. The beads were collected by magnetic separation, and the supernatant was discarded, leaving enough liquid to cover the beads and prevent drying. 450 $\mu$ l of antibody in borate buffer was added to the tube containing the magnetic beads. The tubes were incubated for 1 hour at room temperature with constant rotation using a GyroMini rotating platform. The beads were collected by magnetic separation, and the supernatant was discarded. The beads were resuspended with 500  $\mu$ l of borate buffer, and incubated for 2 minutes at room temperature on a rotator platform. The beads were collected by magnetic separation, and the supernatant was discarded. The resuspension

with borate buffer was repeated once. The beads were resuspended with 450  $\mu$ l of borate buffer, and 2.5 mg of room temperature dimethyl pimelimidate (Sigma Aldrich) was added. The tubes were incubated on a platform rotator for 30 minutes at room temperature. The beads were collected by magnetic separation, and the supernatant was discarded. The beads were resuspended with 500  $\mu$ l of ethanolamine buffer (0.2M ethanolamine in PBS, pH = 8.0). The tubes were incubated for 30 minutes at room temperature on a rotator platform. The beads were collected by magnetic separation, and the supernatant was discarded. The beads were resuspended with 500  $\mu$ l of ethanolamine buffer, and incubated at room temperature on a rotator platform for 2 hours. The beads were collected by magnetic separation, and the supernatant was discarded. The beads were washed with 500  $\mu$ l of phosphate buffered saline (PBS). The beads were collected by magnetic separation, and the supernatant was discarded. The beads were resuspended in 50  $\mu$ l of PBS.

### *C. Co-immunoprecipitation*

Five-hundred  $\mu$ l of precleared whole cell, nuclei, or cytoplasmic lysates were added to tubes containing the cross-linked antibody and beads. The tubes were gently vortexed, and incubated overnight at 4°C with constant rotation using a GyroMini rotating platform. The beads were collected by magnetic separation, and the supernatant was discarded. The pellet wash was washed by resuspending with 500  $\mu$ l of non-denaturing lysis buffer, and incubating on a rotator platform for 5 minutes at room temperature. The washing steps were repeated twice.

## 4.8 Western Blot

### A. *Sample preparation*

For analysis of subcellular localization, 100  $\mu$ l of 4X Laemmli's SDS (reducing) sample buffer (Boston BioProducts) was added to tubes containing either whole cell or nuclei lysates; 50  $\mu$ l of 4X Laemmli's SDS sample buffer was added to tubes containing cytoplasmic contents. One-hundred fifty  $\mu$ l of 4X Laemmli's SDS sample buffer was added to tubes containing immunoprecipitates. All tubes were boiled for 5 minutes. Beads were collected by magnetic separation, the supernatants collected and placed in new microcentrifuge tubes. All tubes were incubated at 4°C for 20 minutes with constant rotation using a GyroMini rotating platform, and then stored at -20°C.

### B. *Gel electrophoresis and transfer*

Equal volumes of samples were resolved on 8 – 10 % SDS PAGE gels under denaturing and reducing conditions. A Multicolor Protein Ladder (Fermentas) and a Precision Plus Dual Standard (BioRad) were used as molecular weight standards. After electrophoresis, proteins were transferred from gels to nitrocellulose membranes for 2.5 hours at 100 Volts.

### C. *Immunoblotting*

Nitrocellulose membranes (BioRad) containing proteins were incubated in blocking buffer (5% milk in TBST) for 1 hour at room temperature on a rotator platform. Blots were probed with primary antibodies specific for GR, HDACs 1, 2, and 3, NCoR, and SMRT; the same antibodies



used for co-immunoprecipitation were used for immunoblotting. Antibodies were diluted in blocking buffer using the following dilutions (Ab:blocking buffer): 1:500 for GR, 1:1000 for HDACs 1, 2, and 3, NCoR, and SMRT. Blots were probed with primary antibodies overnight at 4°C with constant rotation using a GyroMini rotating platform. Blots were washed three times with washing buffer (1X TBST) by incubating on a rotating platform for 5 minutes. Blots were then probed with goat anti-rabbit IgG HRP-conjugated antibody (Millipore 12-348) as a secondary. Blots were washed four times with washing buffer by incubating on a rotating platform for 5 minutes.

Blots were visualized using Supersignal West Pico chemiluminescent reagents (Fisher), and were developed on blue biofilm (BioRad).

#### *D. Quantification of Western Blot*

Films of western blots were scanned to a computer, and blot density was quantified using Image J software. Purity of nuclear and cytoplasmic fractions was determined by blotting for LaminB1 (AbCam ab16048), which is restricted to the nuclear envelope, and GAPDH (Cell Signaling 2118), which is localized to the cytosol. Nuclear fractions were more than 90% pure, and cytoplasmic fractions were more than 85% pure.

### **4.9 Statistical Analysis**

For determination of subcellular localization of GR and HDACs 1, 2, and 3, three independent experiments were conducted. Results are presented as mean  $\pm$  standard error of the mean, with N = 3. Quantitative data was analyzed by two-tailed, two sample, homoscedastic Student's T-test. Values with  $p < 0.05$  were considered statistically significant.

#### 4.10 Buffers and Solutions

Phosphate Buffered Saline (PBS): 100 ml 10X PBS (Invitrogen) and 900 ml Millipore water

Cell Lysis Buffer (per tube): 200  $\mu$ l ProteoJET cell lysis buffer (Fermentas), 2  $\mu$ l ProteoJET 0.1M DTT, and 2  $\mu$ l protease inhibitor cocktail (Sigma Aldrich).

Nuclei Wash Buffer (per tube): 1000  $\mu$ l ProteoJET nuclei washing buffer, 30  $\mu$ l 0.1M DTT, and 2  $\mu$ l protease inhibitor cocktail.

Nuclei Storage Buffer (per tube): 150  $\mu$ l ProteoJET nuclei storage buffer, 7.5  $\mu$ l 0.1M DTT, and 2  $\mu$ l protease inhibitor cocktail.

Non-denaturing Lysis Buffer (for 100ml): 4ml of 0.5M Tris-HCl, 2.75ml of 5M NaCl, 10ml glycerol, 1ml NP-40, 400 $\mu$ l of 0.5M EDTA, and fill to 100 ml with Millipore water. Each tube requires 500  $\mu$ l of non-denaturing lysis buffer with 2  $\mu$ l protease inhibitor cocktail added just prior to use.

Borate Buffer (for 50 ml): dissolve 125 mg boric acid in 10 ml Millipore water and dissolve 765 mg in 40 ml Millipore water. Mix the two solutions, and adjust the pH to 9.0.

Ethanolamine Buffer (for 50 ml): 633.4  $\mu$ l ethanolamine, fill to 50 ml with PBS, and adjust pH to 8.0 with HCl.

Ammonium Persulfate (APS): 1 g ammonium persulfate (Fisher) and 10 ml Millipore water.

8% SDS-PAGE gel: 2.0 ml ProtoGel 30% (Fisher), 1.875 ml 4X Resolving Buffer (Fisher), 3.54 ml Millipore water, 75  $\mu$ l APS, and 7.5  $\mu$ l Temed (Fisher).

10% SDS-PAGE gel: 2.5 ml ProtoGel 30%, 1.875 ml 4X Resolving Buffer (Fisher), 3.04 ml Millipore water, 75  $\mu$ l APS, and 7.5  $\mu$ l Temed.

Stacking gel: 260  $\mu$ l ProtoGel 30%, 500  $\mu$ l Stacking Buffer (Fisher), 1.22 ml Millipore water, 10  $\mu$ l APS, and 2  $\mu$ l Temed.

1X TBST (for 1 L): 100 ml 10X TBST (Boston BioProducts) and 900 ml Millipore water.

5% Milk Blocking Solution (for 50 ml): 2.5 g powdered milk and fill to 50 ml with 1X TBST.

Western Blot Washing Buffer: 1X TBST solution

## CHAPTER FIVE

### RESULTS

#### **5.1 Comparative analysis of natural killer cell activity (NKCA) of the YT-Indy cell line with and without dexamethasone treatment**

The ability of dexamethasone (Dex) to affect YT-Indy lytic activity was evaluated using a standard chromium release assay. YT-Indy cells were treated with dexamethasone ( $10^{-7}M$ ) for 4, 8, 12, or 24 hours. This concentration of Dex was previously determined to be optimal<sup>9</sup>. Dex- and non-treated YT-Indy cells were then incubated for 4 hours with  $Cr^{51}$ -labeled cancer cell line K562 at effector to target ratios of 10 to 1, 20 to 1, and 30 to 1. Supernatants containing radioactivity released by the cancer cells was collected, and the radioactivity was determined. The results are presented in figure 7.

At the 4 hour time point, lytic activity of YT-Indy cells was reduced from 54.33 lytic units (LU) to 43.10 LU with dexamethasone treatment. Lytic activity was reduced from 66.40 LU to 33.74 LU with 8 hours of Dex treatment. With 12 hours of Dex treatment, a reduction in lytic activity from 68.77 LU to 20.47 LU was observed. At the 24 hour time point, Dex treatment reduced lytic activity from 50.59 LU to 12.08 LU. The greatest reduction in lytic activity occurred with 24 hours of dexamethasone treatment, but decreased lytic activity was observed with as little as 4 hours of dexamethasone treatment. Dex treatment had no effect on the viability of the YT-Indy cell line. While decreased lytic activity was observed at all time points tested, statistical difference ( $p < 0.05$ ) between non-treated and Dex-treated cells was observed at 8, 12, and 24-hour time points. Overall, the data demonstrate that dexamethasone decreases lytic activity of YT-Indy cells in a time-dependent manner.

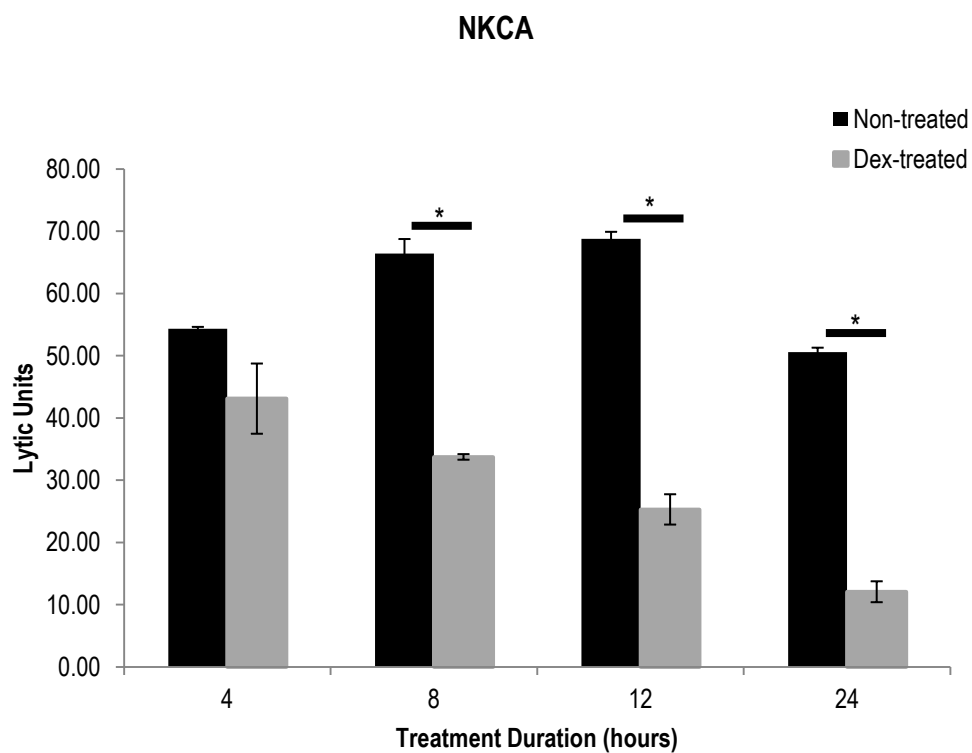


Figure 7. NKCA assay results. ( $n = 3$ ) Each bar represents the lytic units associated with each treatment condition. Each condition was performed in triplicate. Untreated YT-Indy cells are represented by black bars, and dexamethasone-treated cells are represented by grey bars. The data were analyzed using a student's t-test to calculate the probability of a significant difference between the non-treated and Dex-treated conditions. The \* denotes statistical difference ( $p < 0.05$ ) in lytic activity between untreated and Dex-treated cells. Statistically significant decreases in lytic activity due to dexamethasone were observed for treatment durations of 8 hours ( $p = 0.0002$ ), 12 hours ( $p = 0.00008$ ), and 24 hours ( $p = 0.00003$ ). Values are presented as means  $\pm$  SEM.

## 5.2 Comparative analysis of the subcellular localization of glucocorticoid receptor (GR) during dexamethasone treatment

Subcellular localization of GR was assessed in nuclear and cytoplasmic fractions extracted from dexamethasone-treated and non-treated YT-Indy cells. The presence of GR within nuclear and cytoplasmic fractions was determined by Western analysis, using an antibody specific for glucocorticoid receptor. A representative immunoblot from an SDS-PAGE gel is shown in figure 8 A. The density of the protein bands appearing on film was quantified using ImageJ software. The total level of GR within the cell was calculated from the average level GR within the nucleus and the cytoplasm. Figure 8 B displays the percentage of the total cellular GR that is present in either fraction at each time point.

Glucocorticoid receptor is 97 kDaltons. In non-treated YT-Indy cells, GR is found in both the cytoplasm (figure 8 A, lane 2) and the nucleus (lane 1), with the majority present in the cytoplasm (74%, as indicated in figure 8 B). Dexamethasone induces a shift in the proportion of total cellular glucocorticoid receptor found in the nucleus. With 2 hours of Dex treatment, a small increase in the percentage of GR within the nucleus (from 26% in non-treated cells to 34% with 2 hours of Dex) is observed. The greatest increase in GR found within the nucleus occurs at 4 hours of Dex treatment, when 69% of all GR within the cell exists in the nucleus. The change in the levels of GR within the nucleus at 4 hours as compared to untreated cells is statistically significant ( $p = 0.0142$ ). At the 8 hour time point, GR localization returns to levels similar to that of untreated cells, with only 30% of total GR present in the nucleus. Dexamethasone induces a shift in glucocorticoid receptor location to favor nuclear localization at 4 hours of treatment. With 24 hours of treatment, GR is found in approximately equal levels (data not shown).

### Subcellular Localization of GR

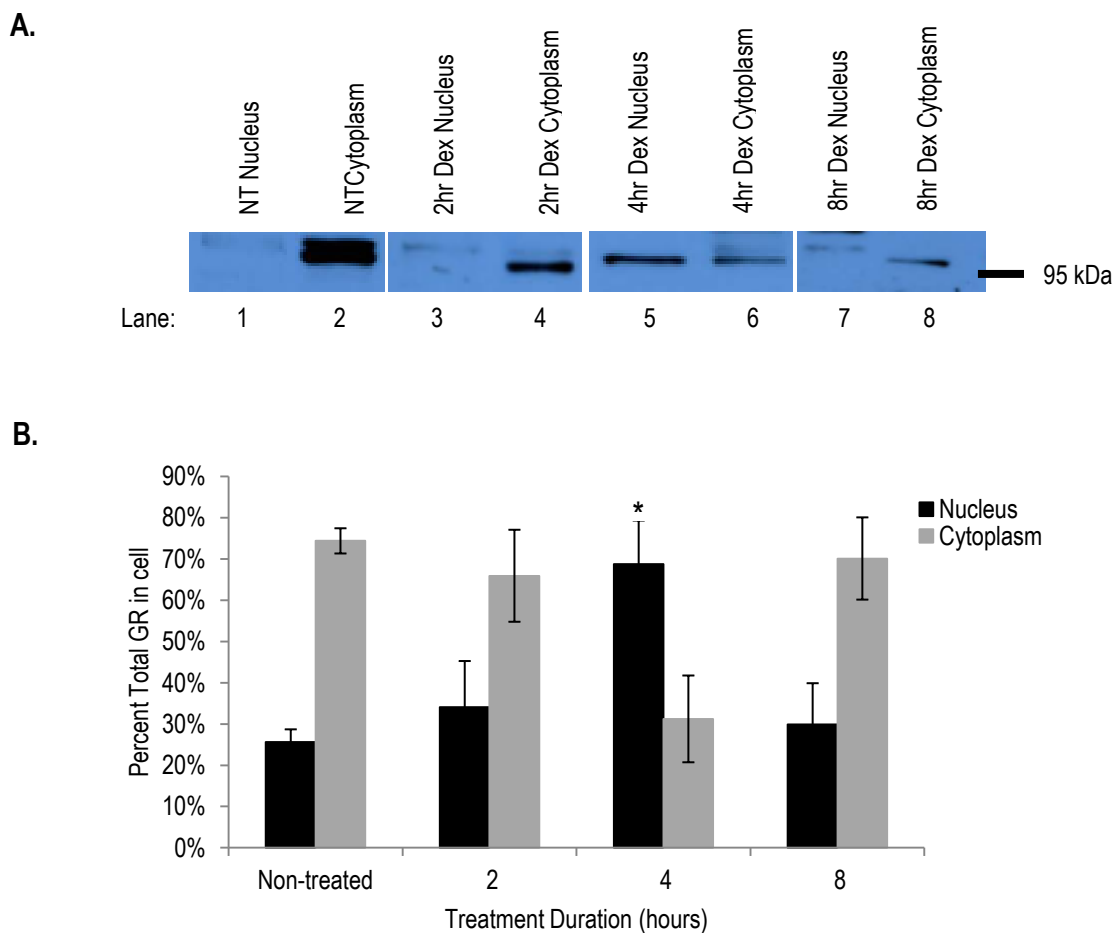


Figure 8. Subcellular localization of GR. A. Representative western blot with non-treated nuclear fraction (lane 1), non-treated cytoplasmic fraction (lane 2), nucleus from 2-hour Dex treatment (lane 3), cytoplasm from 2-hour Dex treatment (lane 4), nucleus from 4-hour Dex treatment (lane 5), cytoplasm from 4-hour Dex treatment (lane 6), nucleus from 8-hour Dex treatment (lane 7), and cytoplasm from 8-hour Dex treatment (lane 8) probed for GR. GR is 97kDa; blot is marked at 95kDa. B. Blot density quantified using ImageJ software. ( $n = 3$ ) Each bar represents the percent of total GR within the cell that is present in either the nucleus or cytoplasm. Nuclear fractions are represented by black bars; cytoplasmic fractions are represented by grey bars. In non-treated cells, 74% of the total GR is present in the cytoplasm. The largest increase in GR found in the nucleus occurs with 4 hours of Dex treatment; the \* denotes statistical difference ( $p < 0.05$ ) in the level of GR in nucleus between 4 hour treatment and non-treated cells. Values are presented as means  $\pm$  SEM.

### 5.3 Comparative analysis of subcellular localization of HDACs 1, 2, and 3 during dexamethasone treatment

Subcellular localization of HDACs 1, 2, and 3 was also assessed using nuclear and cytoplasmic extracts from YT-Indy cells treated for 0, 2, 4, and 8 hours with dexamethasone. The location of HDACs in nuclear or cytoplasmic fractions was determined by immunoblotting with antibodies specific for HDAC1, HDAC2, and HDAC3. Each time point was performed in triplicate. The density of protein bands appearing on film was quantified using ImageJ software. The total cellular level of each HDAC was calculated as the sum of the nuclear and cytoplasmic levels.

#### A. HDAC1

Figure 9 A is a best example western blot of HDAC1. Lanes 1 and 2 display HDAC1 in the nucleus and cytoplasm, respectively, of untreated cells, while lanes 3 – 8 are from Dex-treated cells. HDAC1 is a 65 kDa protein that is present in both cellular fractions of YT-Indy cells, regardless of dexamethasone treatment.

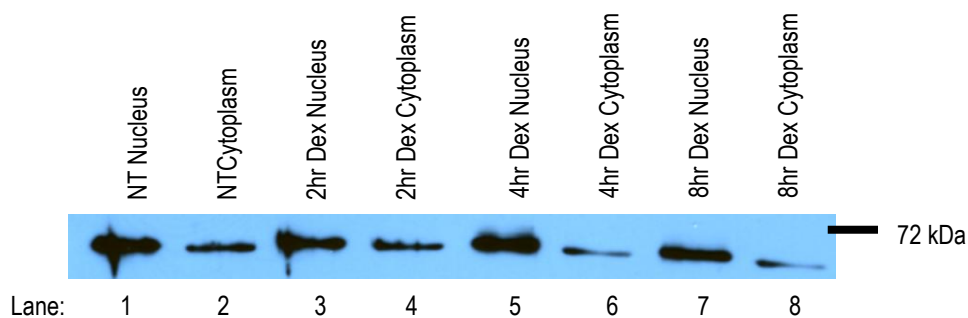
Figure 9 B is more representative of the data, as it presents the average proportion of HDAC1 in the subcellular compartments. In untreated cells, 56% of total cellular HDAC1 is nuclear. On average, dexamethasone increases the proportion of HDAC1 present in the nucleus with 2 and 4 hour treatments; at 2 hours, 76% of HDAC1 is in the nucleus, and 70% is nuclear at 4 hours (figure 9 B). The increase in nuclear HDAC1 observed with 2 hours of Dex treatment is statistically significant ( $p = 0.0107$ ).

Dexamethasone induces HDAC1 to favor nuclear localization with 2 and 4 hours of treatment. However, at 8 hours of treatment, HDAC1 is found in equal proportions in either compartment, a distribution similar to untreated cells.



### Subcellular localization of HDAC1

A.



B.

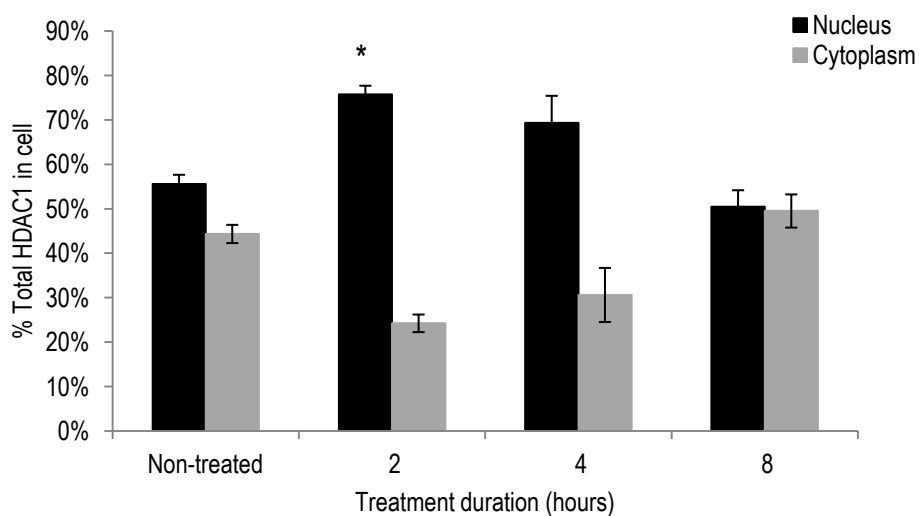


Figure 9. Subcellular localization of HDAC1. A. Representative western blot with non-treated nuclear fraction (lane 1), non-treated cytoplasmic fraction (lane 2), nucleus from 2-hour Dex treatment (lane 3), cytoplasm from 2-hour Dex treatment (lane 4), nucleus from 4-hour Dex treatment (lane 5), cytoplasm from 4-hour Dex treatment (lane 6), nucleus from 8-hour Dex treatment (lane 7), and cytoplasm from 8-hour Dex treatment probed for HDAC1. HDAC1 is 65kDa; blot is marked at 72kDa. B. Blot density quantified using ImageJ software. (n = 3) Each bar represents the percent of total HDAC1 within the cell that is present in either the nucleus or cytoplasm. Nuclear fractions are represented by black bars; cytoplasmic fractions are represented by grey bars. The \* denotes statistical difference ( $p < 0.05$ ) in the level of GR in nucleus between 2 hour treatment and non-treated cells. Values are presented as means  $\pm$  SEM.

## *B. HDAC2*

HDAC2's best representative western blot is depicted in figure 10 A. HDAC2 is a 55 kDa protein that is present in both nuclear (lane 1) and cytoplasmic (lane 2) fractions of untreated YT-Indy cells, as well as the nucleus (lanes 3, 5, and 7) and cytoplasm (lanes 4, 6, and 8) of Dex-treated cells. Figure 10 B is more representative of the data, as it is the average of quantified levels of GR. On average, HDAC2 is divided almost equally between the nucleus and cytoplasm in YT-Indy cells (figure 10 B); 52% of all HDAC2 in the cell is nuclear. Dexamethasone initially induces a statistically significant ( $p = 0.033$ ) increase in the proportion of HDAC2 in the nucleus at 2 hours, with 71% of HDAC2 found in the nucleus. However, continued Dex treatment finds the HDAC2 divided almost equally between the nucleus (47%) and cytoplasm (53%) at 4 hours, and increasing the cytoplasmic proportion (to 58%) at 8 hours.

### Subcellular localization of HDAC2

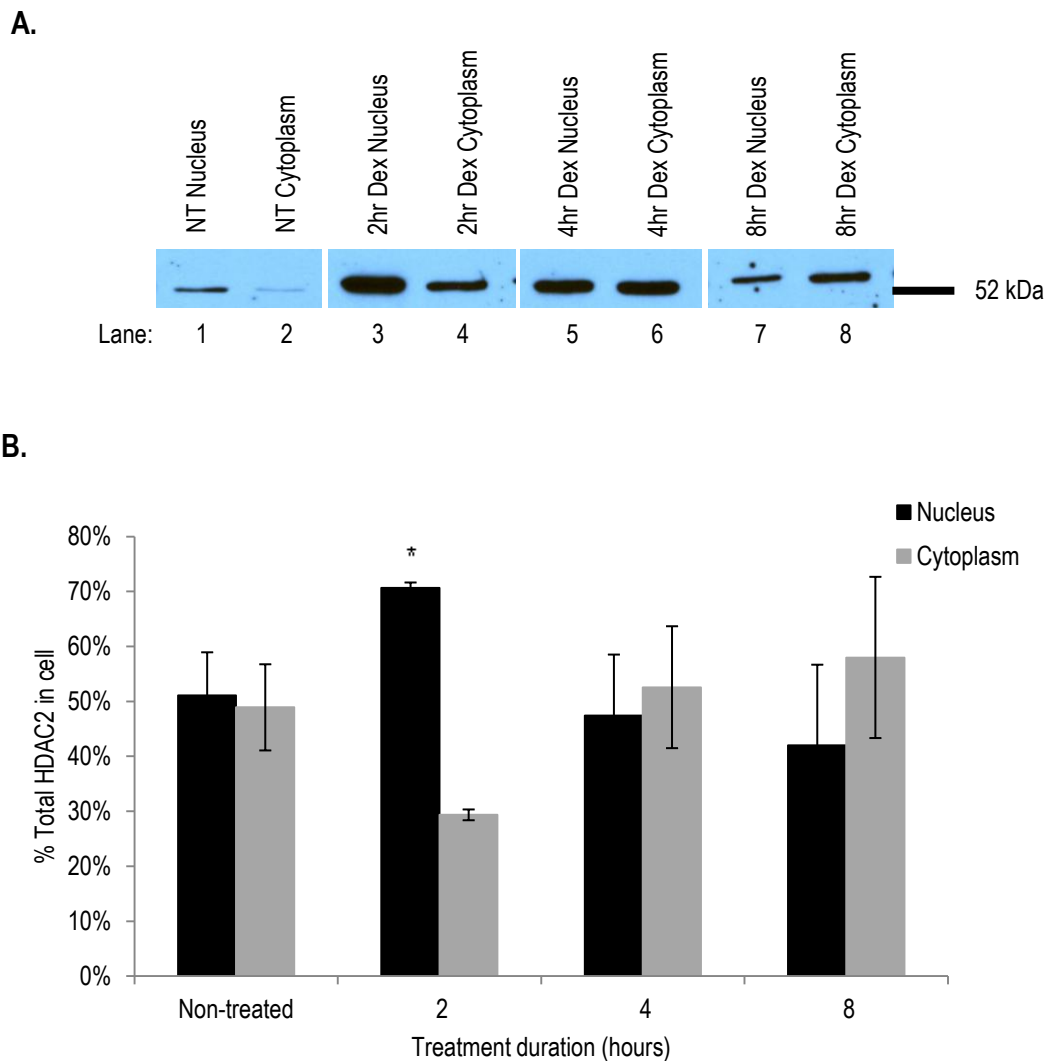


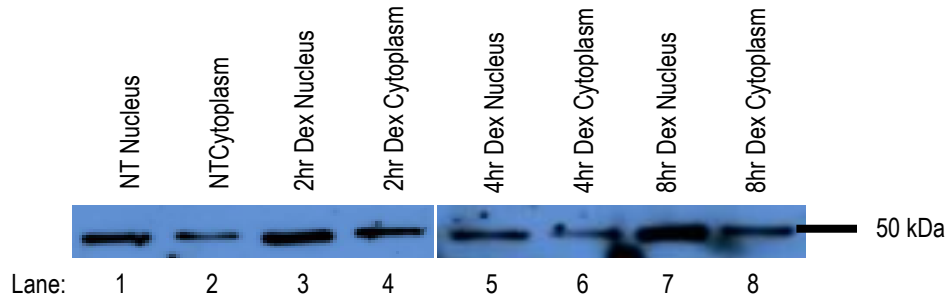
Figure 10. Subcellular localization of HDAC2. A. Representative western blot with non-treated nuclear fraction (lane 1), non-treated cytoplasmic fraction (lane 2), nucleus from 2-hour Dex treatment (lane 3), cytoplasm from 2-hour Dex treatment (lane 4), nucleus from 4-hour Dex treatment (lane 5), cytoplasm from 4-hour Dex treatment (lane 6), nucleus from 8-hour Dex treatment (lane 7), and cytoplasm from 8-hour Dex treatment probed for HDAC2. HDAC2 is 55kDa; blot is marked at 52kDa. B. Blot density quantified using ImageJ software. (n = 3) Each bar represents the percent of total HDAC2 within the cell that is present in either the nucleus or cytoplasm. Nuclear fractions are represented by black bars; cytoplasmic fractions are represented by grey bars. The \* denotes statistical difference ( $p < 0.05$ ) in the level of GR in nucleus between 2 hour treatment and non-treated cells. Values are presented as means  $\pm$  SEM.

### C. HDAC3

Figure 11 A is a best example western blot for HDAC3. Lanes 1 and 2 display HDAC3 in the nucleus and cytoplasm, respectively, of untreated cells, while lanes 3 – 8 are from Dex-treated cells. HDAC3 is a 49 kDa protein that, like HDACs 1 and 2, is present in both the nucleus and cytoplasm of both untreated and Dex-treated cells. Figure 11 B is more representative of the data, as it presents the average proportion of GR in the subcellular compartments. In general, dexamethasone treatment had little effect on subcellular localization of HDAC3. In untreated cells, 64% of total cellular HDAC3 is in the nucleus. Similarly, 57% to 66% of total HDAC3 is within the nucleus of cells treated with dexamethasone. This trend is displayed in the representative blot (figure 11 A) as well. Therefore, dexamethasone treatment does not impact the subcellular localization of HDAC3.

### Subcellular localization of HDAC3

A.



B.

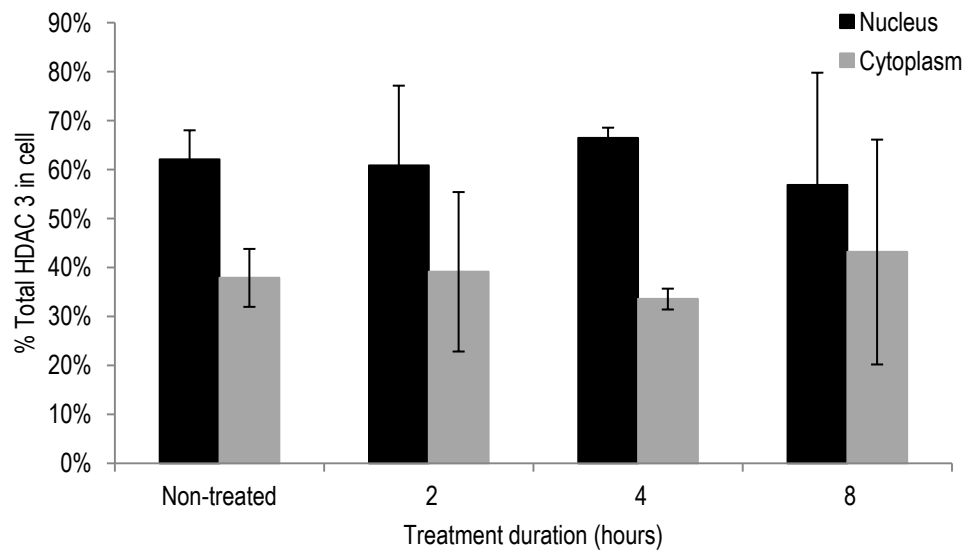


Figure 11. Subcellular localization of HDAC3. A. Representative western blot with non-treated nuclear fraction (lane 1), non-treated cytoplasmic fraction (lane 2), nucleus from 2-hour Dex treatment (lane 3), cytoplasm from 2-hour Dex treatment (lane 4), nucleus from 4-hour Dex treatment (lane 5), cytoplasm from 4-hour Dex treatment (lane 6), nucleus from 8-hour Dex treatment (lane 7), and cytoplasm from 8-hour Dex treatment probed for HDAC3. HDAC3 is 49 kDa; blot is marked at 50 kDa. B. Blot density quantified using ImageJ software. (n = 3) Each bar represents the percent of total HDAC3 within the cell that is present in either the nucleus or cytoplasm. Nuclear fractions are represented by black bars; cytoplasmic fractions are represented by grey bars. Dexamethasone treatment does not induce a statistically significant change in subcellular localization of HDAC3. Values are presented as means  $\pm$  SEM.

#### 5.4 Interactions between GR, HDACs, and Corepressor Complexes

Interaction between proteins was assessed by co-immunoprecipitation assays. YT-Indy cells were cultured with dexamethasone for 4 hours. Whole cells were lysed using non-denaturing lysis buffer to maintain protein-protein interactions; thus, proteins bound together at the time of lysis immunoprecipitate together. Lysates were probed with antibodies specific for glucocorticoid receptor and HDACs 1, 2, and 3; antibodies specific for the corepressor complexes NCoR and SMRT were also used to immunoprecipitate. Lysates were also probed with an IgG antibody that is not specific for any cellular proteins as a negative control; this ensures that immunoprecipitated proteins are not interacting with IgG antibodies non-specifically. Immunoprecipitates were examined by SDS-PAGE gel, and immunoblotted for GR, NCoR, SMRT, and HDACs 1, 2, and 3. Figure 12 shows that the IgG antibody (lane 1) does not immunoprecipitate GR, SMRT, NCoR, HDAC1, HDAC2, or HDAC3. Glucocorticoid receptor is present when an antibody specific for GR immunoprecipitates protein (lane 2). Additionally, GR immunoprecipitates with SMRT and HDAC1, but not NCoR, HDAC2, or HDAC3. The antibody specific for SMRT pulls down SMRT, as well as GR and HDAC1 (lane 3). NCoR is the only protein present when lysates were probed with an NCoR-specific antibody (lane 4). The HDAC1-specific antibody immunoprecipitates GR with HDAC1 (lane 5). Only HDAC2 is pulled down by the HDAC2-specific antibody (lane 6). HDAC3 is the only protein present when lysates were probed with an antibody for HDAC3 (lane 7). GR and SMRT immunoprecipitate together, whether a GR-specific antibody or a SMRT-specific antibody is used. HDAC1 and GR also immunoprecipitate together, whether a GR-specific or HDAC1-specific

### Co-immunoprecipitation of Whole Cell Lysates

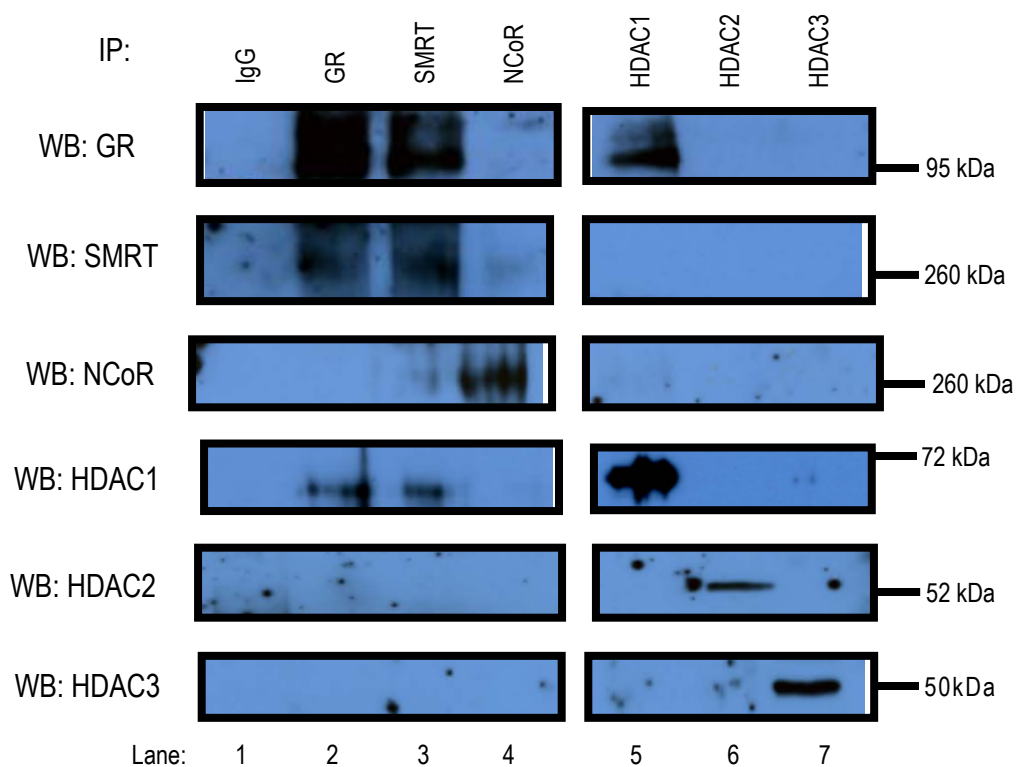


Figure 12. Interaction between GR, corepressor complexes, and HDACs. YT-Indy cells treated with Dexamethasone for 4 hours. Cell lysates were immunoprecipitated with antibodies specific for GR (lane 2), SMRT (lane 3), NCoR (lane 4), HDAC1 (lane 5), HDAC2 (lane 6), and HDAC3 (lane 7); as a negative control, lysates were immunoprecipitated with IgG antibody (lane 1). This is a best representative western blot. No bands appear in lysates immunoprecipitated with IgG (lane 1). SMRT and HDAC1 immunoprecipitate with GR. GR and HDAC1 immunoprecipitate with SMRT (lane 3). GR immunoprecipitates with HDAC1 (lane 5). NCoR Ab only immunoprecipitates NCoR (lane 4), HDAC2 Ab immunoprecipitates only HDAC2 (lane 5), and HDAC3 Ab only pulls down HDAC3 (lane 7).

antibody was used. While a SMRT-specific antibody is capable of immunoprecipitating HDAC1, an HDAC1-specific antibody does not immunoprecipitate SMRT.

As sections 5.2 and 5.3 presented, GR and HDAC1 are present in both the nucleus and cytoplasm of YT-Indy cells. Therefore, to ensure the interaction found in lysates of whole cells were capable of mediating decreases in histone acetylation observed during dexamethasone treatment (supplemental figure 1), the co-immunoprecipitation assay was repeated with nuclear fractions extracted from YT-Indy cells. Nuclei were extracted as previously described (see section 4.5). Nuclei were lysed using the same non-denaturing lysis buffer as whole cells to ensure the preservation of protein-protein interactions. Nuclear lysates were probed with a non-specific IgG antibody as a negative control, as well as antibodies specific for GR, SMRT, and HDAC1, as those proteins were shown to interact in whole cells. Figure 13 demonstrates that no proteins were pulled down with the non-specific IgG antibody (lane 1). Similar to whole cell lysates, the GR-specific antibody pulled down GR, SMRT, and HDAC1 (lane 2) in nuclear lysates. Both GR and HDAC1 were immunoprecipitated with SMRT (lane 3), and HDAC1 immunoprecipitated both GR and SMRT (lane 4). Co-immunoprecipitations of proteins found in nuclear extracts confirmed that GR interacts with SMRT and HDAC1, and suggests that GR is recruiting the corepressor SMRT, as well HDAC1 during dexamethasone treatment to mediate the deacetylation of histone proteins.



### Co-immunoprecipitation of Nuclear Lysates

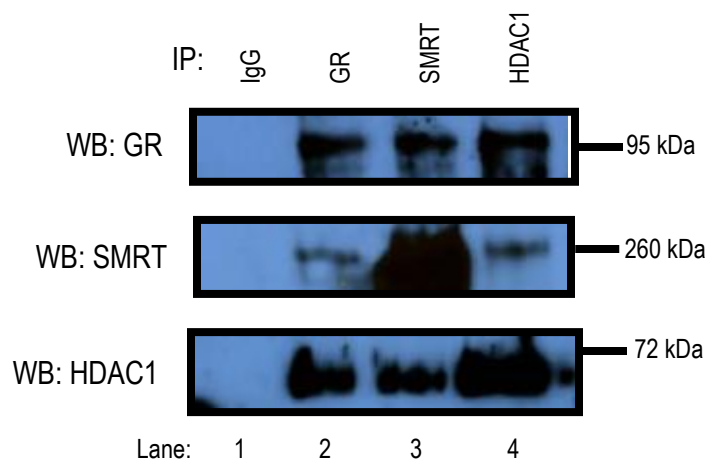


Figure 13. Interaction among GR, SMRT, and HDAC1. YT-Indy cells were treated with dexamethasone for 4 hours. Nuclear and cytoplasmic fractions were separated, and immunoprecipitated with antibodies specific for GR, SMRT, and HDAC1. This is a best representative western blot. As a negative control, nuclear lysates were immunoprecipitated with IgG (lane 1). GR Ab immunoprecipitates GR, SMRT, and HDAC1 (lane 2). SMRT Ab immunoprecipitates SMRT, GR, and HDAC1 (lane 3). HDAC1 Ab immunoprecipitates HDAC1, GR, and SMRT (lane 4).

## CHAPTER SIX

### DISCUSSION

The data presented demonstrate that the glucocorticoid receptor interacts with HDAC1 and the corepressor complex SMRT within the nucleus of YT-Indy cells during dexamethasone treatment (figure 13). These findings were not entirely unprecedented. Recent work by Qiu *et al.* (2006, 2010) demonstrated that GR and HDAC1 co-precipitate in Dex-treated lysates. Hong *et al.* (2009) determined that GR recruits SMRT to GREs during Dex-treatment. SMRT is also known to bind HDAC1<sup>79</sup>. While such associations have been documented, this work is the first to demonstrate interactions among all three proteins, GR, SMRT, and HDAC1, in an NK-like cell line. Others have shown that GR interacts with HDAC2<sup>37</sup> and HDAC3<sup>78</sup>, as well as NCoR<sup>78</sup>. Contrary to those studies, the data demonstrate that GR does not appear to interact with NCoR, HDACs 2 or 3 in YT-Indy cells during dexamethasone treatment (figure 12).

Some of the reported interactions, including GR binding HDAC1 and GR recruiting SMRT, were found in cell lines expressing these proteins from transfection vectors. While such data should not be discounted, interactions need to be confirmed in non-transfected cells; the data presented here demonstrates that GR binds both HDAC1 and SMRT in a cell line expressing these proteins from the genome. Additionally, the interactions documented in this study were found using a cell line, which can model physiological conditions and allow for development of methods

and materials to test primary cells and cells *ex vivo*, in order to confirm these findings in physiological settings.

The interaction among GR, these corepressor complexes, and these HDACs have been found in a variety of cell types<sup>76-79</sup>, suggesting that recruitment of specific complexes and HDACs by GR may be context dependent. As GR has been shown to interact with both NCoR and SMRT<sup>78</sup>, the preference for one corepressor over the other may be due to differences in the subcellular environment among different cell types. Interaction between hormone nuclear receptors like GR and corepressor complexes depend on a number of factors, including the direct binding between GR and the corepressor's interacting domains, as well as the composition of the corepressor complex. It is feasible that different proteins are part of the SMRT or NCoR complexes in different cell types; perhaps in YT-Indy cells, another protein blocks the sites where GR is capable of binding NCoR, but those sites are available on SMRT. This may also explain SMRT's recruitment of HDAC1 instead of HDACs 2 or 3; the site HDAC1 binds in the SMRT complex may be exposed, while the sites for HDACs 2 or 3 are not in this context.

In the nuclei of YT-Indy cells treated with Dex (figure 13), GR precipitates SMRT and HDAC1 (lane 2), SMRT precipitates GR and HDAC1 (lane 3), and HDAC1 precipitates GR and SMRT (lane 4). This demonstrates that GR binds with both HDAC1 and SMRT; however, the order of binding was not determined. However, HDAC1 only precipitates GR, and not SMRT in Dex-treated whole cells (figure 12, lane 5). This raises the possibility that HDAC1 may be binding GR itself, without SMRT, and from the immunoprecipitation data presented here, the order of interaction cannot be determined. Others have reported direct interactions between GR and

HDAC1<sup>77</sup>. The proposed model suggests that interaction between GR and a corepressor complex, SMRT in this instance, recruits the HDAC, HDAC1 in this instance. The data supports such a model, as all three have been shown to interact, but the possibility still exists that HDAC1 binds GR directly. SMRT may recruit HDAC1 to GR initially, and HDAC1 may bind GR directly after the initial recruitment. The interaction between SMRT and GR may also be maintained after HDAC1 binds GR itself, as SMRT may recruit other factors, perhaps proteins with kinase activity to dephosphorylate histone residues. Further testing is required to determine the order of interaction, as well as to demonstrate GR's recruitment of SMRT and HDAC1 to chromatin specifically.

Another finding of this work is the characterization of the subcellular localization of the glucocorticoid receptor during the first eight hours of treatment (figure 8). As anticipated, the majority of GR is within the cytoplasm of non-treated cells (figure 8A, lane 2 as compared to lane 1). On average, 74% of GR is in the cytoplasm (figure 8B). Unactivated GR (without ligand) is more often found in the cytoplasm; however, unactivated GR is known to shuttle between the cytoplasm and nucleus, depending on the accessibility of its nuclear localization sequence and nuclear retention signal<sup>41,42,44</sup>. This may account for 26% of total cellular GR that is within the nucleus of untreated cells. Additionally, the YT-Indy cell line was cultured in supplemented media, which may contain some factor that may reveal GR's NLS, allowing for translocation into the nucleus in the absence of ligand.

While GR is in the cytoplasm of untreated cells, Dex treatment induces a shift of GR into the nucleus, as early as 2 hours (figure 8A, lane 3). With 4 hours of treatment, a reversal from the untreated condition is observed (figure 8B); the majority of GR is in the nucleus at 4 hours. By 8

hours, the majority of GR returns to the cytoplasm. With 24 hours of treatment, GR is divided equally between the nucleus and cytoplasm (data not shown), indicating that GR continues to shuttle between compartments throughout treatment. GR's presence within the nucleus at 4 hours has been demonstrated previously<sup>80,71</sup>, as has GR's localization in both the nucleus and the cytoplasm during Dex treatment<sup>37</sup>.

The presence of GR within a particular subcellular compartment was determined using both western blot and immunocytochemical analysis. The work presented herein analyzed western blots to quantify the level of GR in each compartment during time points ranging from 0 to 24 hours. The quantitative analysis of GR western blot images encountered some challenges. First, GR is reported to be a 97 kDa protein that undergoes various post-transcriptional modifications, including phosphorylation, acetylation, and ubiquitination<sup>39</sup>, and is known to have up to eight isoforms of varying size<sup>81</sup>. Therefore, several band heights were detected in molecular weight range between 95 kDa and 100 kDa (figure 8A). Acetylation occurs in the cytoplasm prior to translocation into nucleus<sup>30</sup>, which may account for the doublet that appears in the cytoplasmic fraction of untreated cells (lane 2, figure 8A), where GR molecules exist in both the acetylated and unacetylated forms. Transport of liganded GR occurs to the acetylated forms only; thus, only the higher molecular weight band, the acetylated form, is seen in the nuclear fraction of these untreated cells (lane 1, figure 8A). Furthermore, in the cytoplasm of cells treated with Dex, GR's ligand, the unacetylated predominates (lane 4, 6, 8), as the acetylated form would translocate into the nucleus upon binding to ligand, which is abundant in the Dex-treated cells. In addition to varying molecular weights, the quantities of GR between time points are not consistent; the level

found in the untreated cells appears to be much greater than the levels in Dex-treated cells.

Dexamethasone is known to decrease the level of GR within the cell by both inhibiting transcription of the GR locus<sup>39</sup> as well as by increasing proteosomal degradation of GR<sup>45</sup>.

In addition to the subcellular localization of GR, HDACs 1, 2, and 3 were evaluated in YT-Indy cells. As figure 9 depicts, HDAC1 is present in both the nucleus (56%) and cytoplasm (45%) of untreated cells, which is consistent with the literature<sup>82</sup>. Dex initially increases the proportion of HDAC1 found in the nucleus at 2 and 4 hours of treatment. At 8 hours of treatment, HDAC1's subcellular localization returns to the pattern found in untreated cells. To date, the effect of dexamethasone treatment on the subcellular localization of HDAC1 has yet to be presented in literature.

As previously stated, HDAC1 is known to exist in both the nucleus and the cytoplasm; HDAC1 requires a shuttle protein for export from the nucleus<sup>59</sup>. The initial increase in HDAC1 in the nucleus during the first 4 hours of Dex treatment may be caused by preventing interaction between HDAC1 and its shuttle protein. HDAC1 is known to interact with many multi-protein complexes including ligand bound GR. It is conceivable that interactions between HDAC1 and GR or other complexes may prevent association with its shuttle protein. As GR dissociates from HDAC1 to exit the nucleus by 8 hours, HDAC1's shuttle protein may bind and escort HDAC1 to the cytoplasm, returning the protein to localization similar to untreated cells.

HDAC2 is also found in both the nucleus (52%) and cytoplasm (48%) of untreated YT-Indy cells (figure 10), as is consistent with the literature<sup>82</sup>. Dex significantly increases the proportion of

HDAC2 in the nucleus at 2 hours (71%), followed by a return to a more equal distribution between both compartments at 4 and 8 hours of treatment.

Nuclear HDAC2 peaks at 2 hours and subsequently decreases; this initial increase coincides with the increase observed with HDAC1. HDACs 1 and 2 are known to associate with each other<sup>78</sup> in multiple protein complexes; thus, the initial retention of HDAC1 may also result in the initial increase in HDAC2 in the nucleus. Then, as increasing levels of ligand bound GR enters the nucleus (peaking at 4 hours of treatment), GR recruitment of HDAC1 may cause HDAC1 to dissociate from HDAC2. Upon interacting with GR, HDAC1 is acetylated, which decreases interaction with HDAC2<sup>79</sup>.

As determined previously<sup>82</sup>, HDAC3 is present in both the nucleus and cytoplasm of YT-Indy cells (figure 11). HDAC3 favors nuclear localization (57% - 66%) in both untreated and Dex-treated cells at all time points, indicating that dexamethasone does not impact the subcellular localization of HDAC3, unlike HDACs 1 and 2. While HDACs 1 and 2 are often reported to be bound together in the nucleus<sup>58</sup>, HDAC3 is not localized with either HDAC 1 or 2<sup>58</sup>. It is possible that GR's recruitment of HDAC1 impacts HDAC2 localization patterns as they are often associated in the nucleus<sup>58,78,79</sup>, but not HDAC3 due to the lack of HDAC1 and HDAC3 binding.

While dexamethasone treatment impacts the localization of HDACs 1 and 2, the data presented demonstrate that HDACs 1, 2, and 3 are all present in the nucleus when GR's nuclear localization peaks at 4 hours. Therefore, all three HDACs are available to interact with GR during dexamethasone treatment, and the impact of these HDACs on GR cannot be ruled out by changes

in localization alone. However, the retention of HDAC1 in the nucleus overlaps the time point with peak levels of nuclear GR, perhaps creating optimal conditions to allow for interaction between these two proteins.

The findings presented confirm that dexamethasone inhibits the natural killer cell activity of the YT-Indy cell line (figure 7). While this trend is well-established in many cell types in the literature<sup>5,6,9,72,73</sup>, the data here confirms that the phenomenon extends to the YT-Indy line as well. Dex significantly decreases the ability of YT-Indy cells to lysis target tumor cells in a time dependent manner as early as 8 hours, with the greatest inhibition observed with 24 hours of treatment.

The lytic activity of YT-Indy cells is enhanced over time by incubating in culture media (figure 7). A significant increase in NK cell activity is observed between 4 and 8 hours of culture. The increased NKCA can be contributed to the presence of fetal bovine serum in the media, as it has previously been shown that cytotoxic activity of NK cells is enhanced by fetal bovine serum<sup>96</sup>. Fetal bovine serum contains numerous cytokines, including IL-2, IL-6, and IL-12, which are known to activate NK cells<sup>97</sup>. Activation of NK cells increases the production of cytokines and effector molecules<sup>97</sup>, including granzymes and perforin, which contribute to NK cytotoxic activity. Fetal bovine serum also contains low levels of IgG, which activates NK cells via the Fc receptor<sup>97</sup>. Culturing in fetal bovine serum has been shown to continuously increase NK cell cytolytic activity over time<sup>96</sup>. From the data presented in figure 7, YT-Indy cytolytic activity is enhanced by culturing with fetal bovine serum, similar to human NK cells.

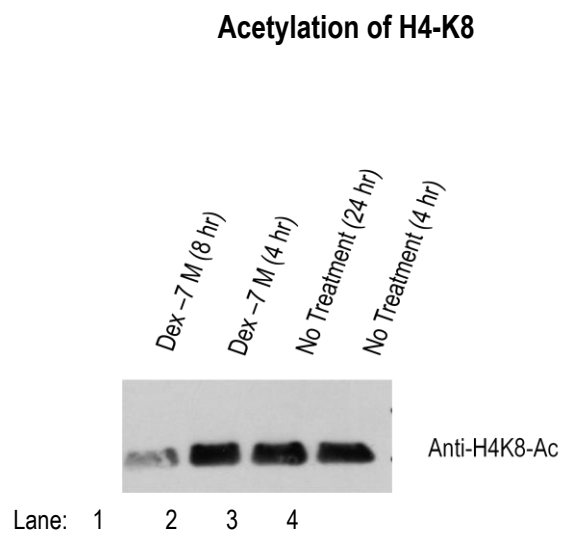


In addition to the findings presented, Dex treatment has been shown to diminish secreted and intracellular levels of both perforin and IFN- $\gamma$  in another NK-like cell line<sup>9</sup>. Treatment of YT-Indy cells with Dex also reduced acetylation of the H4-K8 residue with 8 hours of treatment (supplemental figure 1). Previous work demonstrated that acetylation of H4-K8 residues in the promoter regions of IFN- $\gamma$  and perforin genes was also decreased by dexamethasone treatment<sup>9</sup>.

Taken together with these additional findings, the data presented within suggest that glucocorticoids, like dexamethasone, enter the cell and induce translocation of the glucocorticoid receptor into the nucleus, maximally at 4 hours of treatment. Within the nucleus, GR recruits SMRT and HDAC1, which deacetylates H4-K8 residues in the promoter regions of effector genes, including perforin and IFN- $\gamma$ . The decrease in acetylation of gene promoters results in fewer effector molecules produced and secreted. Fewer effector molecules results in reductions in the ability of NK cells to lyse target cells.

The experimental approach and data presented here can only suggest that HDAC1 is the enzyme responsible for the deacetylation of H4-K8 reported. Further studies are required to determine if HDAC1 binds, either directly or indirectly, to promoter regions of NK cell effector genes. Additionally, HDAC1's enzymatic activity in YT-Indy cells during dexamethasone treatment must also be tested. Furthermore, histone deacetylases are not the only factors to impact histone acetylation status, as histone acetyltransferases are responsible for making the acetylation mark. GR has also been reported to inhibit the activity of HAT complexes<sup>34</sup>; additional testing is required to determine the contributions of HDACs versus HATs to the decrease in histone acetylation levels during Dex treatment.

**APPENDIX A:**  
**SUPPLEMENTAL FIGURES**



Supplemental figure 1. Acetylation of H4-K8. YT-Indy cells were cultured in the presence and absence of dexamethasone for 4, 8, and 24 hours. Cell lysates were analyzed by immunoblot, using an antibody specific for acetylated H4-K8. No change in the level of H4-K8 acetylation between untreated cells at 4 hours (lane 4) or 24 hours (lane 3). No difference in H4-K8 acetylation is observed between untreated cells (lanes 3 and 4) and 4 hour treatment (lane 2). At 8 hours of Dex treatment (lane 1), H4-K8 acetylation is decreased.

Courtesy Karen Krukowski (unpublished data).

## BIBLIOGRAPHY

1. Witek-Janusek, L., Gabram, S., and Mathews, H. L. (2007). Psychologic stress, reduced NK cell activity, and cytokine dysregulation in women experiencing diagnostic breast biopsy. *Psychoneuroendocrinology* 32, 22-35.
2. Stark, D. P., and House, A. (2000). Anxiety in cancer patients. *Br J Cancer* 83, 1261-1267.
3. Witek-Janusek, L., and Mathews, H. L. (2000). Stress, Immunity, and Health Outcomes. In *Handbook of Stress, Coping, and Health: Implications for Nursing Research, Theory, and Practice*, V. Rice, ed. (Thousand Oaks, Sage Publications), pp. 47-67.
4. Witek-Janusek, L., Albuquerque, K., Chroniak, K. R., Chroniak, C., Durazo-Arvizu, R., and Mathews, H. L. (2008). Effect of mindfulness based stress reduction on immune function, quality of life and coping in women newly diagnosed with early stage breast cancer. *Brain Behav Immun* 22, 969-981.
5. Barnes, P. J. (1995). Anti-inflammatory mechanisms of glucocorticoids. *Biochem Soc Trans* 23, 940-945.
6. Schoneveld, O., and Cidlowski, J. A. (2007). Glucocorticoids and immunity: mechanisms of regulation. In *Psychoneuroimmunology*, R. Ader, ed. (Burlington, MA, Elsevier Academic Press), pp. 45-61.
7. Kagoshima, M., Wilcke, T., Ito, K., Tsaprouni, L., Barnes, P. J., Punchard, N., and Adcock, I. M. (2001). Glucocorticoid-mediated transrepression is regulated by histone acetylation and DNA methylation. *Eur J Pharmacol* 429, 327-334.
8. Mishra, N., Brown, D. R., Olorenshaw, I. M., and Kammer, G. M. (2001). Trichostatin A reverses skewed expression of CD154, interleukin-10, and interferon-gamma gene and protein expression in lupus T cells. *Proc Natl Acad Sci U S A* 98, 2628-2633.
9. Krukowski, K., Eddy, J., Kosik, K. L., Konley, T., Janusek, L. W., and Mathews, H. L. (2011). Glucocorticoid dysregulation of natural killer cell function through epigenetic modification. *Brain Behav Immun* 25, 239-249.
10. Beck, I. M., Vanden Berghe, W., Vermeulen, L., Yamamoto, K. R., Haegeman, G., and De Bosscher, K. (2009). Crosstalk in inflammation: the interplay of glucocorticoid receptor-based mechanisms and kinases and phosphatases. *Endocr Rev* 30, 830-882.

11. American Cancer Society (2007). *Breast Cancer Facts & Figures 2007-2008* (Atlanta: American Cancer Society, Inc.).
12. Kiecolt-Glaser, J. K., McGuire, L., Robles, T. F., and Glaser, R. (2002). Emotions, morbidity, and mortality: New Perspectives from Psychoneuroimmunology. *Annu Rev Psychol* 53, 83-107.
13. Luecken, L. J., and Compas, B. E. (2002). Stress, coping, and immune function in breast cancer. *Ann Behav Med* 24, 336-344.
14. Maraste, R., Brandt, L., Olsson, H., and Ryde-Brandt, B. (1992). Anxiety and depression in breast cancer patients at start of adjuvant radiotherapy. Relations to age and type of surgery. *Acta Oncol* 31, 641-643.
15. Northouse, L. L. (1992). Psychological impact of the diagnosis of breast cancer on the patient and her family. *J Am Med Womens Assoc* 47, 161-164.
16. Shapiro, S.L., et al., *Quality of life and breast cancer: relationship to psychosocial variables*. *J Clin Psychol*, 2001. 57(4): p. 501-19.
17. Shapiro, S. L., Lopez, A. M., Schwartz, G. E., Bootzin, R., Figueredo, A. J., Braden, C. J., and Kurker, S. F. (2001). Quality of life and breast cancer: relationship to psychosocial variables. *J Clin Psychol* 57, 501-519.
18. Spiegel, D. (1997). Psychosocial aspects of breast cancer treatment. *Semin Oncol* 24, S1-36-S31-47.
19. Bower, J. E., Ganz, P. A., and Aziz, N. (2005). Altered cortisol response to psychologic stress in breast cancer survivors with persistent fatigue. *Psychosom Med* 67, 277-280.
20. Sephton, S. E., Sapolsky, R. M., Kraemer, H. C., and Spiegel, D. (2000). Diurnal cortisol rhythm as a predictor of breast cancer survival. *J Natl Cancer Inst* 92, 994-1000.
21. Yehuda, R., Boisoineau, D., Lowy, M. T., and Giller, E. L., Jr. (1995). Dose-response changes in plasma cortisol and lymphocyte glucocorticoid receptors following dexamethasone administration in combat veterans with and without posttraumatic stress disorder. *Arch Gen Psychiatry* 52, 583-593.
22. Yehuda, R., Teicher, M. H., Trestman, R. L., Levengood, R. A., and Siever, L. J. (1996). Cortisol regulation in posttraumatic stress disorder and major depression: a chronobiological analysis. *Biol Psychiatry* 40, 79-88.

23. Yehuda, R., Kahana, B., Binder-Brynes, K., Southwick, S. M., Mason, J. W., and Giller, E. L. (1995). Low urinary cortisol excretion in Holocaust survivors with posttraumatic stress disorder. *Am J Psychiatry* 152, 982-986.
24. Yehuda, R. (1998). Psychoneuroendocrinology of post-traumatic stress disorder. *Psychiatr Clin North Am* 21, 359-379.
25. Miller, G. E., Chen, E., and Zhou, E. S. (2007). If it goes up, must it come down? Chronic stress and the hypothalamic-pituitary-adrenocortical axis in humans. *Psychol Bull* 133, 25-45.
26. Eisen, M. (2011). Understanding stress. Yang-Sheng: Cultivate Qi for Body, Mind, and Spirit. 21 Feb 2011, nv., np.
27. Chrousos, G. P. (2000). The role of stress and the hypothalamic-pituitary-adrenal axis in the pathogenesis of the metabolic syndrome: neuro-endocrine and target tissue-related causes. *Int J Obes Relat Metab Disord* 24 Suppl 2, S50-55.
28. Clark, Textbook of Endocrinology, 1992.
29. Torpy, D. J., and Ho, J. T. (2007). Corticosteroid-binding globulin gene polymorphisms: clinical implications and links to idiopathic chronic fatigue disorders. *Clin Endocrinol (Oxf)* 67, 161-167.
30. Nicolaides, N. C., Galata, Z., Kino, T., Chrousos, G. P., and Charmandari, E. The human glucocorticoid receptor: molecular basis of biologic function. *Steroids* 75, 1-12.
31. Gross, K. L., and Cidlowski, J. A. (2008). Tissue-specific glucocorticoid action: a family affair. *Trends Endocrinol Metab* 19, 331-339.
32. Ito, K., Ito, M., Elliott, W. M., Cosio, B., Caramori, G., Kon, O. M., Barczyk, A., Hayashi, S., Adcock, I. M., Hogg, J. C., and Barnes, P. J. (2005). Decreased histone deacetylase activity in chronic obstructive pulmonary disease. *N Engl J Med* 352, 1967-1976.
33. Reichardt, H. M., Tuckermann, J. P., Gottlicher, M., Vujic, M., Weih, F., Angel, P., Herrlich, P., and Schutz, G. (2001). Repression of inflammatory responses in the absence of DNA binding by the glucocorticoid receptor. *Embo J* 20, 7168-7173. De Bosscher, 2003
34. Ito, K., Barnes, P. J., and Adcock, I. M. (2000). Glucocorticoid receptor recruitment of histone deacetylase 2 inhibits interleukin-1beta-induced histone H4 acetylation on lysines 8 and 12. *Mol Cell Biol* 20, 6891-6903.

35. Islam, K. N., and Mendelson, C. R. (2008). Glucocorticoid/glucocorticoid receptor inhibition of surfactant protein-A (SP-A) gene expression in lung type II cells is mediated by repressive changes in histone modification at the SP-A promoter. *Mol Endocrinol* 22, 585-596.
36. Ito, K., Jazrawi, E., Cosio, B., Barnes, P. J., and Adcock, I. M. (2001). p65-activated histone acetyltransferase activity is repressed by glucocorticoids: mifepristone fails to recruit HDAC2 to the p65-HAT complex. *J Biol Chem* 276, 30208-30215.
37. Geng, C. D., and Vedeckis, W. V. (2005). c-Myb and members of the c-Ets family of transcription factors act as molecular switches to mediate opposite steroid regulation of the human glucocorticoid receptor 1A promoter. *J Biol Chem* 280, 43264-43271.
38. Duma, D., Jewell, C. M., and Cidlowski, J. A. (2006). Multiple glucocorticoid receptor isoforms and mechanisms of post-translational modification. *J Steroid Biochem Mol Biol* 102, 11-21. Hache, 2000
39. Savory, J. G., Hsu, B., Laquian, I. R., Giffin, W., Reich, T., Hache, R. J., and Lefebvre, Y. A. (1999). Discrimination between NL1- and NL2-mediated nuclear localization of the glucocorticoid receptor. *Mol Cell Biol* 19, 1025-1037.
40. Freedman, N. D., and Yamamoto, K. R. (2004). Importin 7 and importin alpha/importin beta are nuclear import receptors for the glucocorticoid receptor. *Mol Biol Cell* 15, 2276-2286.
41. Walther, R. F., Lamprecht, C., Ridsdale, A., Groulx, I., Lee, S., Lefebvre, Y. A., and Hache, R. J. (2003). Nuclear export of the glucocorticoid receptor is accelerated by cell fusion-dependent release of calreticulin. *J Biol Chem* 278, 37858-37864.
42. Carrigan, A., Walther, R. F., Salem, H. A., Wu, D., Atlas, E., Lefebvre, Y. A., and Hache, R. J. (2007). An active nuclear retention signal in the glucocorticoid receptor functions as a strong inducer of transcriptional activation. *J Biol Chem* 282, 10963-10971.
43. Wallace, A. D., and Cidlowski, J. A. (2001). Proteasome-mediated glucocorticoid receptor degradation restricts transcriptional signaling by glucocorticoids. *J Biol Chem* 276, 42714-42721.
44. Hubbert, C., Guardiola, A., Shao, R., Kawaguchi, Y., Ito, A., Nixon, A., Yoshida, M., Wang, X. F., and Yao, T. P. (2002). HDAC6 is a microtubule-associated deacetylase. *Nature* 417, 455-458.
45. Juan, L. J., Shia, W. J., Chen, M. H., Yang, W. M., Seto, E., Lin, Y. S., and Wu, C. W. (2000). Histone deacetylases specifically down-regulate p53-dependent gene activation. *J Biol Chem* 275, 20436-20443.

46. de Ruijter, A. J., van Gennip, A. H., Caron, H. N., Kemp, S., and van Kuilenburg, A. B. (2003). Histone deacetylases (HDACs): characterization of the classical HDAC family. *Biochem J* 370, 737-749.
47. Khochbin, S., and Wolffe, A. P. (1997). The origin and utility of histone deacetylases. *FEBS Lett* 419, 157-160.
48. Yang, X. J., and Seto, E. (2003). Collaborative spirit of histone deacetylases in regulating chromatin structure and gene expression. *Curr Opin Genet Dev* 13, 143-153.
49. Guenther, M. G., Lane, W. S., Fischle, W., Verdin, E., Lazar, M. A., and Shiekhhattar, R. (2000). A core SMRT corepressor complex containing HDAC3 and TBL1, a WD40-repeat protein linked to deafness. *Genes Dev* 14, 1048-1057.
50. Jones, P. L., Sachs, L. M., Rouse, N., Wade, P. A., and Shi, Y. B. (2001). Multiple N-CoR complexes contain distinct histone deacetylases. *J Biol Chem* 276, 8807-8811.
51. Li, J., Wang, J., Nawaz, Z., Liu, J. M., Qin, J., and Wong, J. (2000). Both corepressor proteins SMRT and N-CoR exist in large protein complexes containing HDAC3. *Embo J* 19, 4342-4350.
52. Underhill, C., Qutob, M. S., Yee, S. P., and Torchia, J. (2000). A novel nuclear receptor corepressor complex, N-CoR, contains components of the mammalian SWI/SNF complex and the corepressor KAP-1. *J Biol Chem* 275, 40463-40470.
53. Wen, Y. D., Perissi, V., Staszewski, L. M., Yang, W. M., Krones, A., Glass, C. K., Rosenfeld, M. G., and Seto, E. (2000). The histone deacetylase-3 complex contains nuclear receptor corepressors. *Proc Natl Acad Sci U S A* 97, 7202-7207.
54. Jee, Y. K., Gilmour, J., Kelly, A., Bowen, H., Richards, D., Soh, C., Smith, P., Hawrylowicz, C., Cousins, D., Lee, T., and Lavender, P. (2005). Repression of interleukin-5 transcription by the glucocorticoid receptor targets GATA3 signaling and involves histone deacetylase recruitment. *J Biol Chem* 280, 23243-23250.
55. Waltregny, D., Glenisson, W., Tran, S. L., North, B. J., Verdin, E., Colige, A., and Castronovo, V. (2005). Histone deacetylase HDAC8 associates with smooth muscle alpha-actin and is essential for smooth muscle cell contractility. *Faseb J* 19, 966-968.
56. Longworth, M. S., and Laimins, L. A. (2006). Histone deacetylase 3 localizes to the plasma membrane and is a substrate of Src. *Oncogene* 25, 4495-4500.



57. Yang, W. M., Tsai, S. C., Wen, Y. D., Fejer, G., and Seto, E. (2002). Functional domains of histone deacetylase-3. *J Biol Chem* 277, 9447-9454.
58. Verdin, E., Dequiedt, F., and Kasler, H. G. (2003). Class II histone deacetylases: versatile regulators. *Trends Genet* 19, 286-293.
59. Dokmanovic, M., Clarke, C., and Marks, P. A. (2007). Histone deacetylase inhibitors: overview and perspectives. *Mol Cancer Res* 5, 981-989.
60. Gallinari, P., Di Marco, S., Jones, P., Pallaoro, M., and Steinkuhler, C. (2007). HDACs, histone deacetylation and gene transcription: from molecular biology to cancer therapeutics. *Cell Res* 17, 195-211.
61. Fry, C. J., and Peterson, C. L. (2001). Chromatin remodeling enzymes: who's on first? *Curr Biol* 11, R185-197.
62. Jepsen, K., and Rosenfeld, M. G. (2002). Biological roles and mechanistic actions of co-repressor complexes. *J Cell Sci* 115, 689-698.
63. Rosenfeld, M. G., Lunyak, V. V., and Glass, C. K. (2006). Sensors and signals: a coactivator/corepressor/epigenetic code for integrating signal-dependent programs of transcriptional response. *Genes Dev* 20, 1405-1428.
64. Cohen, R. N., Putney, A., Wondisford, F. E., and Hollenberg, A. N. (2000). The nuclear corepressors recognize distinct nuclear receptor complexes. *Mol Endocrinol* 14, 900-914.
65. Zamir, I., Harding, H. P., Atkins, G. B., Horlein, A., Glass, C. K., Rosenfeld, M. G., and Lazar, M. A. (1996). A nuclear hormone receptor corepressor mediates transcriptional silencing by receptors with distinct repression domains. *Mol Cell Biol* 16, 5458-5465.
66. Thiagalingam, S., Cheng, K. H., Lee, H. J., Mineva, N., Thiagalingam, A., and Ponte, J. F. (2003). Histone deacetylases: unique players in shaping the epigenetic histone code. *Ann N Y Acad Sci* 983, 84-100.
67. Adcock, I. M. (2001). Glucocorticoid-regulated transcription factors. *Pulm Pharmacol Ther* 14, 211-219.
68. Almawi, W. Y., and Melemedjian, O. K. (2002). Negative regulation of nuclear factor-kappaB activation and function by glucocorticoids. *J Mol Endocrinol* 28, 69-78.
69. Limbourg, F. P., and Liao, J. K. (2003). Nontranscriptional actions of the glucocorticoid receptor. *J Mol Med* 81, 168-174.

70. Holbrook, N. J., Cox, W. I., and Horner, H. C. (1983). Direct suppression of natural killer activity in human peripheral blood leukocyte cultures by glucocorticoids and its modulation by interferon. *Cancer Res* 43, 4019-4025.
71. Gatti, G., Masera, R., Cavallo, R., Sartori, M. L., Delponte, D., Carignola, R., Salvadori, A., and Angeli, A. (1987). Studies on the mechanism of cortisol inhibition of human natural killer cell activity: effects of calcium entry blockers and calmodulin antagonists. *Steroids* 49, 601-616.
72. Yodoi, J., Teshigawara, K., Nikaido, T., Fukui, K., Noma, T., Honjo, T., Takigawa, M., Sasaki, M., Minato, N., Tsudo, M., and et al. (1985). TCGF (IL 2)-receptor inducing factor(s). I. Regulation of IL 2 receptor on a natural killer-like cell line (YT cells). *J Immunol* 134, 1623-1630.
73. Montel, A. H., Bochan, M. R., Hobbs, J. A., Lynch, D. H., and Brahmi, Z. (1995). Fas involvement in cytotoxicity mediated by human NK cells. *Cell Immunol* 166, 236-246.
74. Drexler, H. G., and Matsuo, Y. (2000). Malignant hematopoietic cell lines: in vitro models for the study of natural killer cell leukemia-lymphoma. *Leukemia* 14, 777-782.
75. Tarazona, R., Borrego, F., Galiani, M. D., Aguado, E., Pena, J., Coligan, J. E., and Solana, R. (2002). Inhibition of CD28-mediated natural cytotoxicity by KIR2DL2 does not require p56(lck) in the NK cell line YT-Indy. *Mol Immunol* 38, 495-503.
76. Qiu, Y., Zhao, Y., Becker, M., John, S., Parekh, B. S., Huang, S., Hendarwanto, A., Martinez, E. D., Chen, Y., Lu, H., et al. (2006). HDAC1 acetylation is linked to progressive modulation of steroid receptor-induced gene transcription. *Mol Cell* 22, 669-679.
77. Qiu, Y., Stavreva, D. A., Luo, Y., Indrawan, A., Chang, M., and Hager, G. L. Dynamic interaction of HDAC1 with a glucocorticoid receptor-regulated gene is modulated by the activity state of the promoter. *J Biol Chem* 286, 7641-7647.
78. Hong, W., Banihmad, A., Li, J., Chang, C., Gao, W., and Liu, Y. (2009). Bag-1M inhibits the transactivation of the glucocorticoid receptor via recruitment of corepressors. *FEBS Lett* 583, 2451-2456.
79. Jones, P. L., Sachs, L. M., Rouse, N., Wade, P. A., and Shi, Y. B. (2001). Multiple N-CoR complexes contain distinct histone deacetylases. *J Biol Chem* 276, 8807-8811.
80. Sackey, F. N., Hache, R. J., Reich, T., Kwast-Welfeld, J., and Lefebvre, Y. A. (1996). Determinants of subcellular distribution of the glucocorticoid receptor. *Mol Endocrinol* 10, 1191-1205.

81. Lu, N. Z., and Cidlowski, J. A. (2005). Translational regulatory mechanisms generate N-terminal glucocorticoid receptor isoforms with unique transcriptional target genes. *Mol Cell* 18, 331-342.
82. Keedy, K. S., Archin, N. M., Gates, A. T., Espeseth, A., Hazuda, D. J., and Margolis, D. M. (2009). A limited group of class I histone deacetylases acts to repress human immunodeficiency virus type 1 expression. *J Virol* 83, 4749-4756.
83. Kelly, G. (2010). A review of the sirtuin system, its clinical implications, and the potential role of dietary activators like resveratrol: part 1. *Alt Med Rev* 15, 245-263.
84. Kouzarides, T. (2007). Chromatin modifications and their function. *Cell* 128, 693-705.
85. Strahl, B. D., and Allis, C. D. (2000). The language of covalent histone modifications. *Nature* 403, 41-45.
86. Jenuwein, T., and Allis, C. D. (2001). Translating the histone code. *Science* 293, 1074-1080.
87. Jones, P. A., and Baylin, S. B. (2007). The epigenomics of cancer. *Cell* 128, 683-692.
88. Sterner, D. E., and Berger, S. L. (2000). Acetylation of histones and transcription-related factors. *Microbiol Mol Biol Rev* 64, 435-459.
89. Cuthbert, G. L., Daujat, S., Snowden, A. W., Erdjument-Bromage, H., Hagiwara, T., Yamada, M., Schneider, R., Gregory, P. D., Tempst, P., Bannister, A. J., and Kouzarides, T. (2004). Histone deimination antagonizes arginine methylation. *Cell* 118, 545-553.
90. Zhang, Y., and Reinberg, D. (2001). Transcription regulation by histone methylation: interplay between different covalent modifications of the core histone tails. *Genes Dev.* 15, 2343-2360.
91. Nowak, S. J., and Corces, V. G. (2004). Phosphorylation of histone H3: a balancing act between chromosome condensation and transcriptional activation. *Trends Genet.* 20, 214-220.
92. Nelson, C. J., Santos-Rosa, H., and Kouzarides, T. (2006). Proline isomerization of histone H3 regulates lysine methylation and gene expression. *Cell* 126, 905-916.
93. Nathan, D., Ingvarsdottir, K., Sterner, D. E., Bylebyl, G. R., Dokmanovic, M., Dorsey, J. A., Whelan, K. A., Krsmanovic, M., Lane, W. S., Meluh, P. B., Johnson, E. S., and Berger, S. L. (2006). Histone sumoylation is a negative regulator in *Saccharomyces cerevisiae* and shows dynamic interplay with positive-acting histone modifications. *Genes Dev.* 20, 966-976.

94. Shilatifard, A. (2006). Chromatin modifications by methylation and ubiquitination: implications in the regulation of gene expression. *Annu. Rev. Biochem.* 75, 243-269.
95. Cosgrove, M. S., and Wolberger, C. (2005). How does the histone code work? *Biochem. Cell Biol.* 83, 468-476.
96. Zielska, J. V., and Golub, S. H. (1976). Fetal calf serum-induced blastogenic and cytotoxic responses of human lymphocytes. *Cancer Res* 36, 3842-3848.
97. Whiteside, T. L., and Herberman, R. B. (1994). Role of human natural killer cells in health and disease. *Clin Diag Lab Immunol* 1, 125-133.

## VITA

Kristin Ashley Bush was born on December 7, 1983 to George and Lynn Bush in Blue Island, Illinois. She attended Benedictine University in Lisle, Illinois, and graduated with a Bachelor of Science in Molecular Biology in May of 2006. After college, she worked in the research and development division at Alberto Culver, Inc., formulating hair care products. In August of 2008, Kristin entered the graduate program in Microbiology and Immunology at Loyola University; she joined the lab of Dr. Herbert Mathews, PhD and Dr. Linda Witek-Janusek, PhD in July 2009. She received a Master of Science in Microbiology and Immunology in December 2011.